1 **A systematic study into the effect of lignocellulose-derived biofuels on the combustion**

2 **and emissions of fossil diesel blends in a compression ignition engine**

3 *James Frost, Dr Paul Hellier, Prof Nicos Ladommatos*

4

Abstract

6 Screening of a variety of bioderived furanic molecules was performed in order to improve our

7 understanding of how this class of molecules respond during compression-ignition

8 combustion, after blending with diesel fuel. Reducing carbon emissions is possible through

9 the use of "2nd generation" carbon neutral biofuels, the sources of which are from non-edible

10 feedstocks, meaning that competition with food resources is negated. The tested molecules

11 were selected for their potentially more economic and less energy intensive production routes,

12 compared to more conventional alternative diesel fuels.

13 These furan-based molecules were varied in their degree of molecular saturation, their

14 branching and in the addition of an oxygenated functional group. It was found that the

15 molecules liberated from lignocellulosic biomass need to be saturated to achieve stable

16 combustion when blended at a volumetric ratio of 50:50 with fossil diesel. The aromatic ring

17 of a furan molecule was postulated to be difficult to break down and increased the ignition

18 delay substantially. This resulted in a significant increase in carbon monoxide (CO) emissions.

19 Blending with butanol and increasing the proportion of diesel in the blend mitigated this effect,

20 and enabled the effect on emissions of adding furan molecules into a blend to be evaluated

21 with a wider range of candidate molecules. Biofuel combustion produced higher NO_x

22 emissions and particle number, while particle mass decreased compared to the fossil diesel.

23 Between the molecules, an increase in the degree of saturation decreased the ignition delay,

24 which tended to decrease the NO_x emissions and increase the particle mass. Furthermore,

25 the effect of adding alkyl chains to the ring structure tended to increase the molecules'

26 propensity to ignite by providing more radicals during the ignition delay period; longer single

27 chains were more effective compared to numerous shorter chains. It was also noted that the

28   addition of an oxygenated functional group to the molecule decreased the particle mass in all

29   cases. Carbonyl groups decreased the ignition delay period relative to the base molecule while

30   alcohol groups increased this period; in both cases, however, NO_x emissions increased.

31

1. Introduction

33   Transportation accounts for approximately 30% of global greenhouse gas emissions.[1]

34   Current transport methods generally rely on the internal combustion engine and the use of

35   crude oil derivatives, gasoline and diesel - fossil fuels - that are finite and produce carbon

36   dioxide (CO_2) as a product of their combustion to release energy.

37   This sector's contribution to total emissions is not only upon the utilisation of transportation

38   fuels, but also the production process of obtaining crude oil and processing it into fractions

39   that are suitable for combustion in compression or spark ignition engines.[2] Moreover, while

40   the negative impact of burning fossil fuels on the planet is apparent through climate change,

41   other emissions produced from the combustion of fossil fuels, such as nitrous oxides (NO_x),

42   particulates and unburnt hydrocarbons (UHCs), are also of concern. The impact of these

43   emissions is directly upon human health,[3] therefore regulations are stringent in limiting the

44   amount that are produced per km. In Europe, emissions of NO_x are limited to 0.08 g/km for

45   compression ignition engines, and 0.06 g/km for spark ignition engines under the most recent

46   Euro 6 regulations. This is a considerable reduction relative to the limit of 0.18 g/km for

47   compression ignition (diesel) cars established by the Euro 5b regulations 3 years earlier.[4]

48   These new regulations have necessitated the use of exhaust after-treatment and catalytic

49   converters to lower the output of NO_x and PM. However, the disadvantages of these systems

50   are their high cost, since platinum group metals are required,[3] and the necessity of a warm-

51   up period before they can become fully effective.

52   The use of alternatives fuels could result in benefits, both in terms of the harmful emissions

53   produced during combustion from the engine itself as well as reducing upstream carbon

54   emissions, through the use of a carbon neutral feedstock. So-called 'biofuels', which may be

sourced from a variety of feedstocks, are potentially carbon neutral and thus their use can help reduce the overall carbon footprint of transport, even as a minor fuel blending component. While electrification of the automotive industry is currently on-going, there is anticipated to be a continued need for the internal combustion engine in some applications; particularly in heavy-duty vehicles. The use of biofuels has also been shown to mitigate the amount of harmful pollutants produced during combustion, particularly particulate mass, postulated to be due to the reduction in fuel carbon radicals that are responsible for soot formation.[5]

The use of bio-derived fuels is not a new concept, as the first diesel engine produced in 1892 was designed to run on peanut oil.[6] However, 2nd generation biofuels are now emerging as potential fuel blending components based on the lack of competition with food and agriculture for the land to grow the feedstock.[7] This represents the biggest drawback of 1st generation biofuels, such as bioethanol, in which the feedstock can also be used to produce food which, in some countries, is a more immediate priority.[8]

Lignocellulose from non-edible (2nd generation) biomass would appear to be an untapped resource. Consisting of cellulose (40-50%), hemicellulose (25-35%) and lignin (15-20%), hydrolysis into sugar monomers and subsequent dehydration can convert both the cellulose and hemicellulose into 'platform chemicals'.[9] Chief among these platform molecules are hydroxymethylfurfural (HMF) and furfural, obtained via the direct dehydration of C_6 and C_5 sugars respectively. Furfural has been produced since 1921 in a process developed by Quaker Oats, which utilises a homogenous acid catalysts in the form of sulfuric acid.[10] HMF, conversely, became fully commercialised more recently in 2013,[11] and tends to require harsher conditions to liberate as the structure of cellulose is more resilient to acids due to cross-linking between molecules.

Corma et. al investigated the potential of converting these platform chemicals into liquid alkanes that resembles what we know today as diesel range fuel. [9,12–14] However, H_2 pressures of 50 bar, temperatures of 350°C and a platinum based catalyst were required to yield 94.6% alkane from a hydroxyalkylated feedstock processed from biomass through a homogeneous acid catalyst.

The conditions required are detrimental to this route's sustainability on a larger scale. Consequently, selection of molecules that may be obtained further upstream relative to alkane production is advantageous from a cost perspective, though their applicability as diesel fuel blenders is not well understood. From both HMF and furfural, dimethylfuran (DMF) and methylfuran (MF), respectively, can be formed via selective hydrogenation of the carbonyl (and alcohol) groups on these molecules.[9]

Both DMF and MF have been tested in combustion engines due to their high energy density and blending ability, but almost exclusively in gasoline engines due to their low carbon and high octane numbers (119 for DMF and 103 for MF).[15,16] Studies into the use of these as diesel fuel blends are more scarce due to relatively high resistance to autoignitoin.[17–20] Saturated derivatives are arguably more applicable for diesel engines as it has been shown that these are more prone to autoignition with higher cetane numbers,[15,21,22] although some contradictions to this have been found based on the engine operating conditions.[23,24] The main drawback to the use of saturated molecules is the extra processing required; aromatics are obtained from the biomass source, therefore saturation using an additional hydrogen source is required, using heterogenous catalysts. Whether saturated THF derivatives are necessary in diesel engines is not clear. For compression ignition engines, a fuel is required that will auto-ignite due to the release of sufficient radicals at the temperatures and pressures it is exposed to in the combustion chamber. A greater number of hydrogen atoms in the molecule will allow for a greater number of these radicals to be released, which means that higher carbon number, fully saturated molecules are generally used in these engines. Moreover, these molecules tend to be straight chained molecules, rather than branched analogues. Branched alkanes possess longer ignition delays than n-alkanes, primarily due to the reduced rate of isomerisation that takes place in the early-stage combustion phase.[25] Alternatively, furfural may undergo etherification using an alcohol to extend the chain to almost any chain length depending on the alcohol selected. This work has been performed by a number of groups,[26,27] including a spin-off company from Shell,[28] where a road test using t-butoxymethylfurfural (25

110   vol% in commercial diesel) was performed. These tests yielded positive results in

111   demonstrating the ability of the biofuel blend to reduce soot emissions, in this case by 20%.

112   Ultimately, the aim of the current study was to elucidate the combustion attributes best

113   suited to a diesel fuel blending component, taking a furan or THF ring structure obtainable

114   from biomass as a starting point. Partially saturated dihydrofurans (2,3-DHF and 2,5-DHF)

115   were also used to determine any trend with degree of saturation. Methyl, dimethyl and ethyl

116   chain lengths were compared, while the addition of an oxygenated group - an aldehyde,

117   ketone or alcohol functional group – was evaluated.

118   The key features of the analysis were the ignition delay period, heat release rate and

119   emissions. Ignition delay is the simplest parameter on which to consider the molecules'

120   viability as a diesel fuel. Overall, the higher the propensity of auto-ignition (shorter ignition

121   delay- a higher cetane number) the more viable the molecule is for use as a diesel fuel. The

122   use of oxygenated biofuels in combustion engines has shown to be beneficial regarding soot

123   emissions, although NO_x emissions often rise to somewhat counter this benefit. Studies outline

124   that soot emissions are heavily dependent on the amount of oxygen present within the

125   molecule,[29] though a linear reduction is not observed due to the potential impact of oxygenated

126   biofuel molecules on physical properties; the increase in viscosity that the biofuel tends to

127   afford can increase soot emissions due to a poorer mixing rate during the ignition delay period,

128   resulting in more fuel rich zones that can produce pyrolysis products such as soot.[30]

129   Oxygenated molecules vary in their effect on emissions, depending on the type and location

130   of the bond present. Alcohols, for example, increase the ignition delay period substantially,[31]

131   and thus the reduction in soot emissions seen from the combustion of these molecules may

132   be attributed also to the extended mixing period that reduces the aforementioned fuel rich

133   zones.[32] Moreover, ignition delay periods were noted to be longer for a group of n-alcohols

134   when the position of the alcohol group was moved closer to the centre of the molecule, which

135   in turn increased NO_x emissions through a greater degree of pre-mixed combustion. Furans

136   have more recently attracted attention, with MF and DMF used in gasoline[33] and diesel[17,18]

137   blends. As with other oxygenated fuels, an increase in the blend proportion tends to decrease

138   the mass and size of the particulates produced, which can be partially attributed to an increase

139   in the reactivity of the soot particles produced from biofuel combustion. NO_x emissions tend to

140   increase as the furan blend ratio increases due to the longer ignition delays observed.

141   Observation of exhaust emissions also enables conclusions encompassing the overall

142   combustion process to be drawn. CO emissions are indicative of the amount of incomplete

143   combustion occurring, NO_x emissions are generally a result of higher cylinder temperatures,

144   a function of the timing and duration of the ignition delay period, while particulate emissions

145   are dictated by the ability of the fuel and air to mix (as well as the nature of the fuel being

146   used). Aromatic hydrocarbons, typically present in conventional diesel fuel (approximately 10

147   vol% in a general reference fuel[34]) are precursors to soot formation, therefore utilising an

148   aromatic biofuel molecule may increase the amount of soot produced. Moreover, a molecule

149   with more oxygen atoms can potentially enhance the soot oxidation phase post agglomeration

150   and coagulation. There is also the possibility that soot formation itself is disrupted by the

151   addition of an oxygenated fuel molecule; pyrolysis products such as acetylene and

152   unsaturated hydrocarbons are known soot precursors, and form when there is a lack of oxygen

153   available for combustion.[35] Fuel-bound oxygen likely negates this effect or, alternatively,

154   hinders the growth of these precursors into larger molecules, such as polycyclic aromatic

155   hydrocarbons (PAHs) that are intermediates towards particulates.[36]

156   It is clear that there are contrasting effects on the combustion and emissions of oxygenated

157   biofuels within a fossil diesel blend, dependent on the changes in chemical and physical

158   properties induced by the presence of the oxygenated molecule. In order to better understand

159   these changes, a systematic study was performed using a selection of molecules based on a

160   range of platform chemicals, furfural and HMF. Both 50:50 blends and 70:20:10 blends with

161   diesel and butanol were tested. The 50:50 blends with fossil diesel were performed on

162   empirical molecules such as furan and THF, since these fuels blended successfully, without

163   the addition of a butanol co-solvent. For the fuels with longer chains (ethylfuran) or those with

164   an additional oxygen, a consistent ratio of 70 vol% diesel, 20 vol% butanol and 10 vol% furan-

165 derivative was selected to enable a homogenous mixture to form that could produce consistent

166 results during combustion testing.

167

2. Methodology

169 *2.1. Diesel Engine Facility*

170 The research engine, specified in Table 2.1 below, was a direct-injection, custom built, 4-

171 stroke single cylinder compression-ignition engine. The majority of components (cylinder

172 head, intake manifold, fuel injector, piston and connecting rod) were obtained from a 2.0 litre

173 turbocharged diesel engine (Ford Duratorq CD132 130PS). For the engine crank case, a

174 Ricardo Hydra single cylinder crank case was employed; an adaptor plate was required to

175 utilise the head in the single cylinder configuration. A David McClure DC motor dynamometer,

176 capable of motoring the engine up to 5000rpm, was controlled by a Cussons test-bed console.

177 The combustion chamber itself, as stated in Table 2.1, consisted of a ω shaped bowl piston

178 and a flat roof, with two intake and two exhaust valves, and a centrally located injector.

179

180

181 **Table 2.1: Diesel Engine Specifications**

182

Engine Head Model	Ford Duratorq
Engine Crankcase Model	Ricardo Hydra
No. of Cylinders	1
Cylinder Bore (mm)	86
Cylinder Stroke (mm)	86
Swept Volume (cm^3)	499.56
Geometric Compression Ratio	18.3 : 1
Max In-Cylinder Pressure (bar)	150
Piston Bowl Design	Central ω bowl

Fuel Injection Pump	Delphi single-cam radial-piston pump
High-pressure Common Rail	Delphi solenoid controlled (Max 1600 bar)
Diesel Fuel Injector	6-hole solenoid valve injector (Delphi DFI 1.3)
Fuel Injection System	1 µs duration (EMTRONIX EC-GEN 500)
Crank Shaft Encoder	1800 ppr (0.2 CAD resolution)

183

184   Gaseous emissions (CO, CO_2, NO_x) were all measured using a Horiba MEXA 9100H EGR

185   automotive gas analyser. Particulate emissions (size distribution, mass and number) were

186   measured using a particulate spectrometer (Cambustion DMS500). Emissions were sampled

187   approximately 50cm downstream of the exhaust valve, with separated heated lines connecting

188   the exhaust to the gaseous emissions analyser and DMS500 (set at 190°C). Possible

189   measurement error of this equipment, and other instrumentation utilised in these tests, is

190   outlined in table 2.2.

191

192   **Table 2.2: Instrumentation uncertainty**

193

Measurement Type	Measurement Purpose	Manufacturer	Instrumentational Error
Piezoresistive pressure transducer	In-cylinder pressure	Kistler	$\pm0.18\%$
Shaft encoder	Combustion timing	N/A	$\pm0.03\%$
Dynanometer	Engine speed	David McClure Ltd	$\pm2\%$
Infrared	CO/CO_2 emissions	Horiba	$\pm1\%$
Chemiluminescence	NO_x emissions	Horiba	$\pm1\%$

194

195

196

197

198

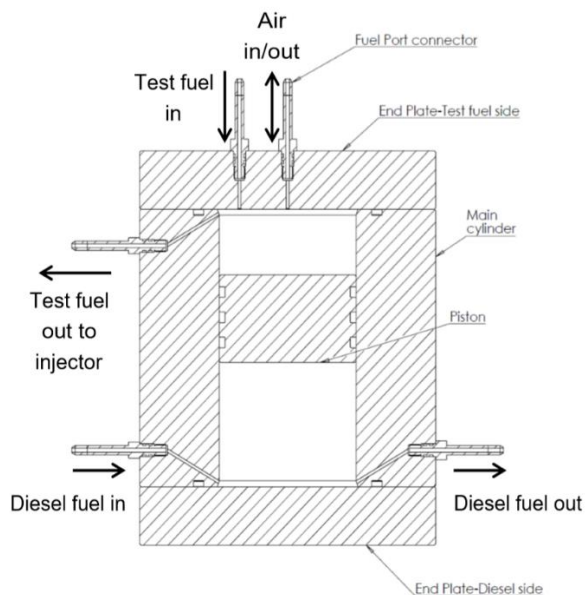199   *2.2.   Fuel System*

200

201

Figure 2.1: Cross sectional view of high pressure fuel system

For the test blends, a novel fuel system was employed for the high pressure, direct injection, of a blend into the combustion chamber. There existed three fundamental issues with using the standard header tank for these fuels; the cost of some of these molecules was such that testing these in the quantities required for the standard system was not economically feasible; secondly, the inability to efficiently purge the header

213 tank from contamination of other fuels meant that residual test fuels would likely render results

214 invalid if ignition properties had varied significantly between sequential fuels. The final problem

215 was that the properties of some of the test fuels, such as viscosity and density, were not

216 suitable to use in the standard common rail system.

217   As a result, the fuel system shown in Figure 2.1 was designed to utilise low amounts of

218 fuel (less than 1L), be easy to clean and reuse for different fuels in relatively quick succession,

219 and bypass the most sensitive components on the standard injection system (such as the fuel

220 pump) that would be most susceptible to corrosion or failure due to a lack of lubricity. A

221 schematic of the fuel circuit is illustrated in figure 2.2, outlining the ability of using diesel from

222 the header tank as a hydraulic fluid, pressurising the test fuel within the high pressure fuel

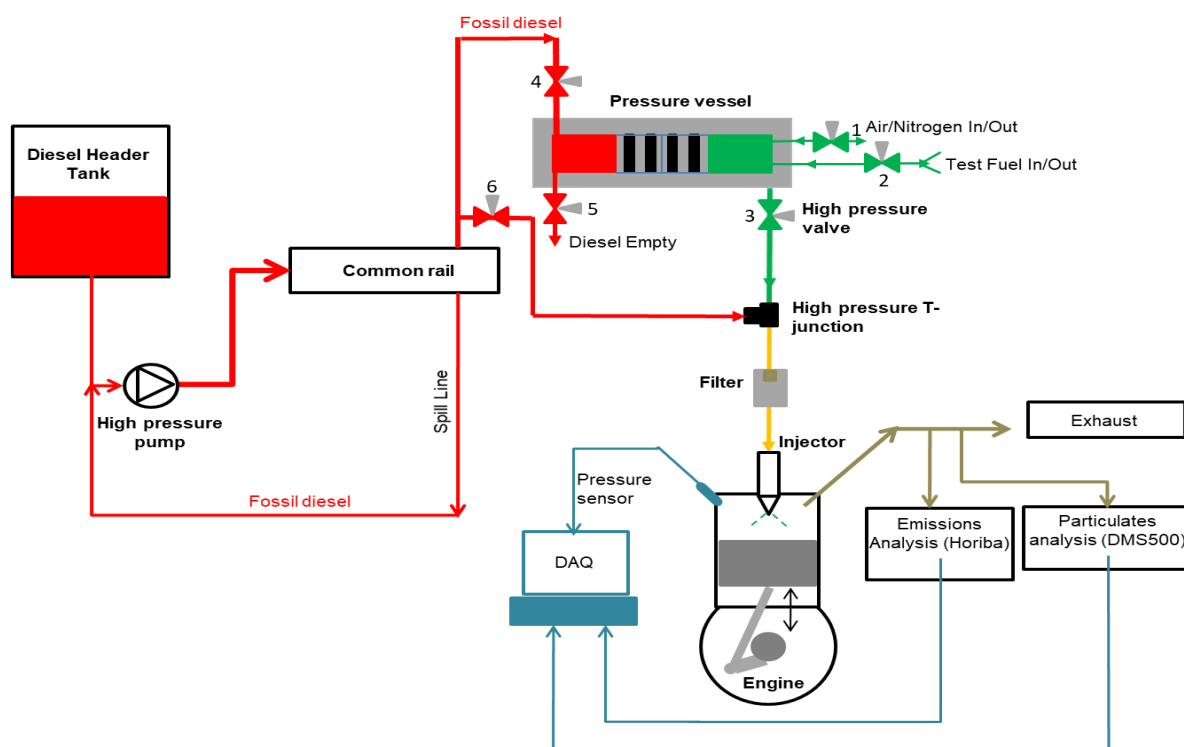223 system, or directly as the injected fuel itself.

224

225

226

227   ***Figure 2.2: Schematic of Experimental setup, including injection directly from the***

228   ***common rail (through valve 6) and via the low volume fuel system***

229

230

231   *2.3.   Fuel Blending*

232

233   A range of fuel molecules, illustrated in Table 2.3, theoretically attainable from biomass,

234   were tested as fuel blends with diesel in the aforementioned CI engine; either in 50:50 volume

235   ratios or 10% in a 70:20:10 volume ratio blend with diesel and n-butanol.

236   Furfural (99%), Furfuryl Alcohol (98%), 2-Acetylfuran (99%), Furan (99%), 2,3-

237   Dihydrofuran (99%), 2,5-Dihydrofuran (97%), Tetrahydrofuran (99.9%), 2-Methylfuran (99%),

238   2,5-Dimethylfuran (99%), 2-Ethylfuran (99%), 2-Methyltetrahydrofuran (99%), 2-

239   Methyltetrahydrofuran-3-one (97%) were all purchased from Sigma Aldrich. 1-Butanol (99%)

240   was purchased from Alfa Aesar and the zero FAME content fossil diesel used was purchased

241   from Haltermann Carless.

Furanic species are hazardous chemicals, therefore all blending was performed within a fume cupboard and subsequent utilisation i.e in the filling and refilling of the fuel system, was undertaken using a full face respirator, nitrile gloves and disposable lab coat.

Blending was performed on a volumetric basis; for example, a 50:50 blend of 200mL would therefore include 100mL of fossil diesel and 100mL of test fuel. Given that some test fuels, particularly heavily oxygenated molecules such as furfural, are highly viscous and polar in nature, a homogenous mixture was not immediately formed when these were added to the fossil diesel and butanol mixture. Subsequently, a magnetic stirrer bar was employed for all blends to ensure that each component had dissolved. It should be noted here that butanol was primarily used for its ability to dissolve the insoluble oxygenated fuels into the diesel fuel; its use as a blending component in diesel fuel is limited due to its low cetane number (15.92).[37]

Stirring was performed for at least 5 minutes or until no visible separation was evident after the mixture was allowed to settle for 1 hour. Before engine tests, the blends were observed and photographed to ensure no separation had transpired before the test fuel was introduced to the engine fuel system. Figure 2.3 below indicates the effect that a lack of stirring had on the blending ability of the furan fuel in fossil diesel.

(a)　　　　　　　　**(b)**

Figure 2.3: Comparison of 50:50 furfuryl alcohol blend with diesel having formed a homogenous mixture (a) and a visibly separated mixture (b)
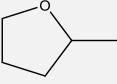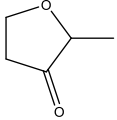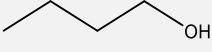
262

263 **Table 2.3: List of Tested Molecules**

264

MOLECULE	ABBREVIATION	BOILING POINT (°C)[38]	DENSITY (G/ML)[38]	OXYGEN CONTENT (%)	(DERIVED) CETANE NUMBER[21,37,39]	LOWER HEATING VALUE (MJ/KG)[15]
Furan	none	31	0.936	11.1	7	-
Methylfuran	MF	63	0.91	8.3	8.9	31.2
Dimethylfuran	DMF	92	0.903	6.7	10.9	33.8
Ethylfuran	EF	92	0.912	6.7	10.2	-
Tetrahydrofuran	THF	66	0.889	7.7	21.9	34.6
2,3-Dihydrofuran	2,3-DHF	54	0.927	9.1	20.0	-
2,5-Dihydrofuran	2,5-DHF	66	0.927	9.1	15.6	-
Furfural	FF	162	1.16	18.2	13.9	-
Furfuryl Alcohol	FA	170	1.135	15.4	10.8	-
Acetylfuran	AF	168	1.098	14.3	-	-

Methyl-tetrahydrofuran	**MTHF**	78	0.86	6.3	22.0	32.8
Methyl-tetrahydrofuran-3-one	**MTHF-3-one**	139	1.034	13.3	-	-
n-butanol	**none**	118	0.81	6.7	15.92	34.4
DIESEL	**none**	150-380	0.85	0	52.2	43.0

265

266

267   *2.4.   Engine Operation*

268

269   For all tests, engine conditions were kept consistent to ensure useful comparison across

270   different blends and molecules, as shown in Table 2.4. Intake temperatures were maintained

271   at 120°C using an inline air heater (Secomak 571), which was placed 330mm upstream of the

272   intake manifold. This temperature was employed to ensure the successful ignition of all test

273   fuels at the engine conditions utilised, while maintaining consistency across samples to ensure

274   comparisons were valid. All engine tests were conducted from a control room; no personnel

275   was allowed to enter the test cell during engine operation.

276

277

278

279

280

281

282

Table 2.4: Engine Operating Conditions

Engine Condition	Steady-state Value
Engine Load	4 bar IMEP
Engine Speed	1200 rpm
Injection Pressure	550 bar
Injection Timing	10 CAD BTDC (except for Diesel:furan and Diesel: MF blend combustion)
Air Intake Pressure	Atmospheric
Air Inlet Temperature	120°C

In order to maintain a constant engine load of 4 bar IMEP, the injection duration was varied between fuels and also between specific tests of the same fuel. This relatively low engine load was used so as to ensure results were more representative of city driving; air pollution is particularly pertinent in urban environments. Furthermore, lower engine loads were hoped to emphasise the impact of fuel molecular structure on combustion emissions; higher engine loads and the higher temperatures associated with these could obscure the subtleties of combustion variances between blends. Moreover, the low amounts of fuel available meant that high injection durations were not feasible for the collection of multiple data points. Table 2.5 shows the range, and mean value, of injection durations required when combusting different fuel blends. Overall, these differences could be attributed to two factors; firstly, different fuel molecules possess different calorific contents for a given mass; more heavily oxygenated fuels tend to possess lower energy densities, and therefore required longer injection durations to maintain the same engine load. Secondly, the physical properties impacted the injection system itself, for example, a highly viscous fuel such as furfuryl alcohol (FA), required a longer injection period since the greater frictional forces present between the fuel and injector components necessitated longer injector opening times for the release of the

same mass of fuel. Moreover, blends with poor lubricity may have resulted in increased friction

between injector components, thus delaying needle movement relative to the control signal.

Table 2.5: Average injection timings for each fuel blend

Fuel Blend	Average Injection Duration (µs)	Injection Duration COV (%)
Furan	762	0.95
MF	757	1.62
DMF	697	2.23
2,3- DHF	684	0.42
2,5- DHF	657	0.72
THF	668	0
MTHF	753	2.89
10% DMF	880	4.95
10% MTHF	860	3.40
10% EF	801	2.36
10% FF	696	0.66
10% FA	713	0.80
10% AF	701	0.24
10% MTHF-3-one	740	0.96
Diesel	**666**	**3.99 (Overall)** **1.53 (Average Daily)**

311

3. **Results and Discussion**

3.1.   Combustion Characteristics

3.1.1.   Degree of Saturation

315

316
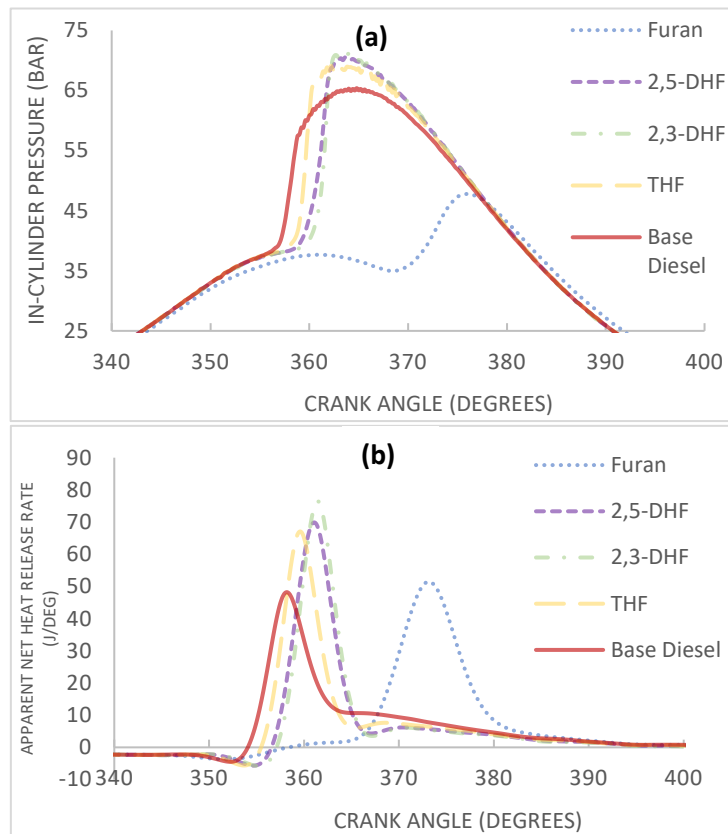
Figure 3.1: In-cylinder pressure (a) and apparent heat release rate (b) of 50:50 Furan:Diesel Blends and Base Diesel, comparing the degree of saturation. Injection timings were held consistently at 10° BTDC (except for the furan blend, where injection was retarded to 19° BTDC to enable combustion)

331   Figure 3.1 shows the in-cylinder pressure and corresponding heat release rate of the

332   various 50:50 furanic fuel:diesel blends, comparing the saturation of the molecule; with furan

333   fully unsaturated (aromatic), DHF partially unsaturated and THF fully saturated.

334   The in-cylinder pressure indicates an earlier release of energy, in the case of pure diesel,

335   compared to the 50:50 furanic fuel:diesel blends, with the combustion retarded approximately

336   2 crank angle degrees (CAD) in the case of THF and the two DHF blends. Meanwhile

337   furan:diesel combustion did not begin until well into the expansion stroke, and once full ignition

338   commenced a significantly lower in-cylinder pressure was reached (Figure 3.1 (a)). Apparent

339   from the heat release of the furan:diesel blend (Figure 3.1 (b)) is that initial combustion

340   commenced at a timing similar to the other blends, but an appreciable increase in heat release

341   is not noted until after 365 CAD. It is postulated that combustion begins in the case of

342   furan:diesel from radicals created purely from the diesel fraction; the aromatic molecule may

343   not have produced radicals readily, and in fact acted as a radical sink. Polyaromatic

344   hydrocarbons are known to quench reaction rates by acting as a sink for hydrogen atoms,[40]

345   and their stability means that they persist for long periods of time, therefore it is not

346   unreasonable to expect a similar phenomenon for these aromatic furan species. Eventually

347   however, with escalating temperatures, furan decomposition begins, the ring opens, releasing

348   radicals, and rapid premixed combustion ensues. Aromatics contain extremely stable π bonds,

349   which makes H-abstraction difficult. Boot[41] notes, however, that once H-abstraction has

350   occurred, and the ring has opened, the bond dissociation enthalpies (BDEs) throughout the

351   molecule decrease and combustion can ensue more rapidly. This may also explain the

352   apparent 2-stage combustion occurring in the case of furan, indicated clearly in Figure 3.1(b)

353   by a slight rise in heat release at 355 CAD, before more significant heat release commences

354   at approximately 366 CAD; it is suggested that, at this timing, the furan component is able to

355   burn.

356
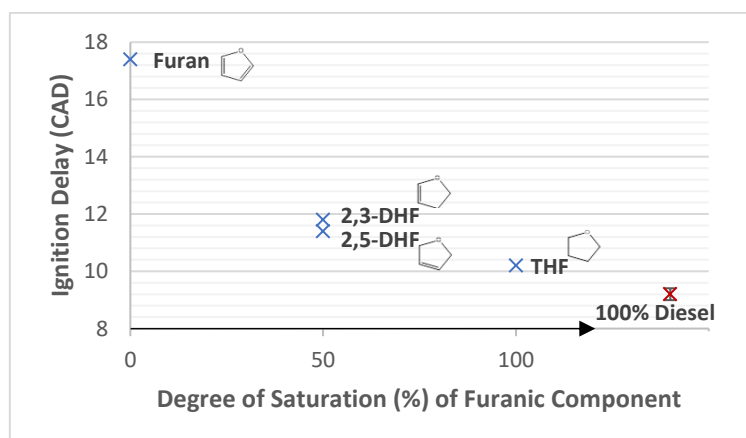
Figure 3.2: Duration of ignition delay of 50:50 vol:vol blends of fossil diesel and furan molecules of varying degrees of saturation (blue cross), also to unblended reference diesel (red dot)

359

360

361

Throughout this work, the ignition delay period is defined by the duration (in CAD) from the timing of fuel injection to the time at which combustion commences (when net heat release becomes positive). Figure 3.2 shows the ignition delay of the 50:50 furan blends and reference diesel, where saturation of the furan molecules increases from left to right. Immediately apparent is that a greater degree of saturation reduces the duration of ignition delay. This is in agreement with previous studies[30,42] whereby a greater degree of saturation has been observed to increase the propensity of a molecule to auto-ignite. The least saturated molecule tested, furan, exhibited the longest ignition delay of 17.4 CAD, while THF, which is fully saturated, possessed an ignition delay of 10.2 CAD (Figure 3.2). Boot[41] explains that H-abstraction on olefins (unsaturated species) produces allyl radicals, which contain delocalised pairs of electrons and therefore are highly stable, slowing down the overall reaction rate. Moreover, Fan[43] provides comparisons of the BDEs of C-H groups for furan, both dihydrofurans and THF; it is noted that the highest BDE, and therefore most difficult H-abstraction, is present in furan. A more saturated molecule also possesses a greater number of hydrogen atoms that may be extracted, therefore the size of the radical pool during the combustion of a more saturated molecule has the potential to be greater. The extended delay period of furan was such that the injection timing needed to be retarded to 19 CAD in order for ignition to occur close enough to TDC that stable combustion could ensue (illustrated in Figure 3.1).

All test blends exhibited longer delay periods than neat diesel, which was anticipated given that the oxygen present within the furan molecules will likely have a negative impact on the rate of early-stage low temperature combustion reaction such as H-abstraction and isomerization. However, it is apparent from these results that the aromaticity has a larger effect on ignition delay than the presence of oxygen within the blends; a difference of 1 CAD exists between base diesel and the THF:diesel blend, but an increase in delay of 1.2-1.8 CAD was observed between the THF:diesel blend and partially unsaturated DHF:diesel blends. A study by Eldeeb[44] compared the ignition delay times of a furan-based molecule- DMF- and the

hydrocarbon isooctane in a shock tube study at temperatures from 1000-1400K, concluding that the latter was considerably more reactive as iso-octane undergoes unimolecular decomposition, which generates radicals early on, while H-abstraction by O_2 is the dominant reaction pathway in the case of DMF.

The difference observed in the ignition delay of the position isomers, 2,3-DHF and 2,5-DHF, was small, at only 0.4 CAD, therefore any conclusions based upon this are stressed as only tentative predictions. According to Sudholt's study;[21] the location of the double bond is important in dictating the cetane number as a result of the change in bond dissociation energies around the rest of the molecule. In the case of 2,3-DHF, it is stated that H-abstraction will first occur on the opposite side of the molecule from the double bond (the double bond linking positions 4 and 5), primarily at the saturated C2 position because the hydrogen atoms at the C1 position are partially stabilised by the lone pairs of electrons on the oxygen. For 2,5-DHF, Sudholt notes that the BDEs are lower for comparable positions 2,3-DHF, which could explain the slightly lower ignition delay in the case of 2,5-DHF in the current study (Figure 3.2). However, it was also suggested that while the position of the double bond in 2,5-DHF results in easier H-abstraction, the subsequent radical is unreactive, which would then hinder further early stage combustion reactions. For this reason, the cetane number calculated by Sudholt (Table 2.3) was higher in the case of 2,3-DHF. While this does not agree with the observed shorter ignition delay of the 2,5-DHF blend (Figure 3.2), these cetane numbers were calculated for pure fuels, and thus the impact of blending with diesel in the current work, and any synergies in the low temperature reaction kinetics of the furans and diesel hydrocarbons, are not accounted for. Furthermore, the ignitability of the fossil diesel is likely to dominate, therefore any differences in auto-ignition between the dihydrofuran blends used here were likely obscured as the differences in calculated cetane number are small.

3.1.2. Number and Length of Alkyl Branching

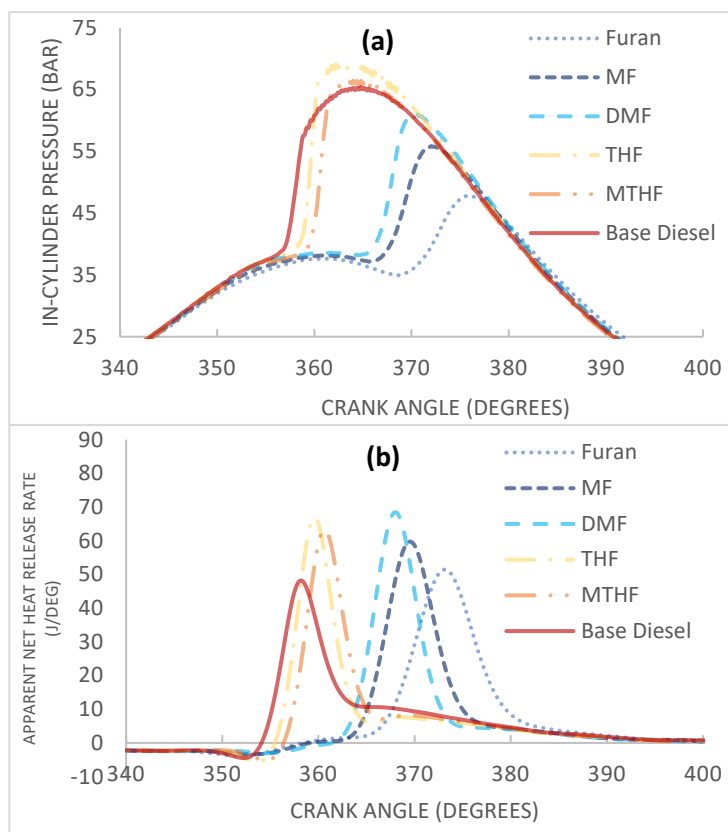Figure 3.3: In-cylinder pressure (a) and apparent net heat release rate (b) of 50:50 Furan:Diesel Blends, comparing the level of molecular branching

A comparison of the furan molecules, of varying alkyl branching, are shown in Figure 3.3. Apparent from in-cylinder pressure and heat release rates is that there was a clear distinction between saturated and aromatic molecules, but the combustion performance was improved with the addition of alkyl groups, with heat release commencing at more favourable conditions (closer to TDC) in the case of DMF compared to MF and furan. From the results of furan, MF and DMF illustrated in Figure 3.3b, it is postulated that the slightly destabilising effect of alkyl chains on an aromatic ring, as well as the easier hydrogen abstraction from the alkyl carbon, likely allowed for a greater pool of radicals to form in the ignition delay phase where early-stage combustion reactions occurred.[21] Furthermore, the additional alkyl chain(s) allow for a

20

445 greater range of reaction pathways in the oxidation or decomposition of these aromatics; early

446 studies concluded that the loss of CO was the only process in furan and MF decomposition,

447 but other pathways were possible in DMF decomposition.[45] More recent investigations

448 determined that H-addition onto the carbon adjacent to the oxygen in furan to produce

449 acetylene was possible. In MF, H-abstraction from the methyl group was dominant, while DMF

450 possessed a high tendency to produce 1,3-cyclopentadiene and benzene- soot precursors.[46–

451 48] Ultimately, the presence of alkyl chains not only improves reaction rates with lower bond

452 dissociation enthalpies,[21] but also increases the number of potential reactions. However,

453 despite the improvement in ignition with alkyl branching, the in-cylinder pressure (Figure 3.3a)

454 indicates combustion is still only occurring in the expansion stroke for the aromatic furan

455 blends, therefore peak pressures and heat release rates are relatively low. The higher peak

456 HRR and peak pressures in the combustion of a more branched molecule are not replicated

457 in the case of saturated THF and MTHF however, though it is suggested that the benefit of

458 adding a methyl branch is not as apparent in fully saturated THF, which possesses good

459 ignition quality, compared to an aromatic that is highly resistant to ignition.

460 MTHF may be expected to produce higher heat release rates than THF, given the slightly

461 longer ignition delay period allowing for more premixing. Since the chemical properties are

462 very similar, the physical properties of the two molecules should also be considered. The lower

463 volatility of MTHF, coupled with a slightly higher density/viscosity, can be observed in the heat

464 release rate traces in Figure 3.4b. MTHF possesses a slightly longer delay period, but this

465 does not see greater premixed combustion and a subsequently higher pHRR. The fact that

466 this is not the case here indicates that, potentially, the mixing rate of MTHF is poorer than that

467 of THF; the more gradual slope of the decreasing trace (between approximately 353 and 355

468 CAD in the Figure 3.4b HRR trace) for MTHF indicates that this vaporisation period is not as
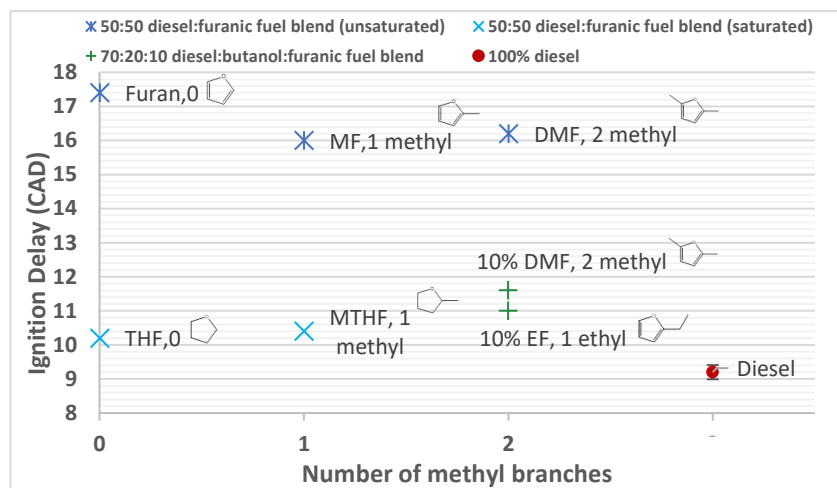
469 rapid.

470

471

472

Figure 3.4: Duration of ignition delay, comparing the level of molecular branching, in both 50:50 (blue star) and 70:20:10 (green cross) blend ratios to diesel (red dot)

Figure 3.4 shows the ignition delay periods of furanic fuel:diesel blends and furanic fuel:butanol:diesel blends, comparing the number and length of alkyl branches present on the furan ring. From furan to MF to DMF, there is an increase in branching, and a slight decrease in ignition delay by 1.4 CAD from furan to MF (it should be noted that an earlier injection timing was used for the furan:diesel and MF:diesel blends in order to attain stable combustion). In the case of the fully saturated furan derivatives, addition of a single methyl branch increased the duration of ignition delay of MTHF relative to THF by 0.2 CAD. Comparing the 10% furan molecule blends, ethylfuran possessed a 0.6 CAD shorter delay period than DMF.

Ultimately, the hydrogen atoms on any side chain of a furan species are considerably easier to remove than on the stable furan ring itself, therefore H-abstraction occurs here initially and, as a result, the ignition delay period is expected to decrease when alkyl chains are applied.[15] The delay period of DMF is longer than that of ethylfuran because the BDEs of the two alkyl branches are equally strong in DMF, whereas, in ethylfuran, Sudholt indicates that the carbon atom between the end of the alkyl chain and the ring carbon will be very reactive (with a BDE of 351kJ/mol, compared to 360.9kJ/mol as the lowest BDE in 2-MF). These results are in agreement with Eldeeb's comparative investigation, where ethylfuran was found to ignite up to six times faster than DMF.[44] This suggests that the second carbon on the alkyl chain has a significant effect on the propensity for a furan species to ignite, and any

furan-based designer molecule should possess at least two carbons on a side chain. Under oxidative conditions, Sudholt suggests that the most prevalent reaction pathway for a furan species is an addition reaction and subsequent ring opening into alkenes, rather than hydrogen abstraction. Since H-abstraction is not the major reaction pathway, adding an additional methyl chain (therefore more H-abstraction sites) may not have a considerable effect.

The ignition delay of THF and MTHF is very similar, 10.2 and 10.4 respectively (Figure 3.4). While Sudholt notes that ignition behaviour is dictated by the side chain of a THF molecule, this does not hold true between THF and MTHF, since the differences in BDEs are not significant between methyl and ring carbons, and the addition of a methyl chain does not alter the C-H bond strength of the ring carbons relative to base THF.[21] For all THFs, it is claimed that hydrogen abstraction first occurs on the carbon connected to the oxygen and any side chain present. Ultimately, hydrogen abstraction occurs at either the C2 or C5 position in THF, and primarily the C2 position in 2-MTHF. Since the location of radical attack is unchanged in MTHF relative to THF, the reaction pathway and rate is likely very similar for both molecules, and therefore the ignition delay is not significantly affected.
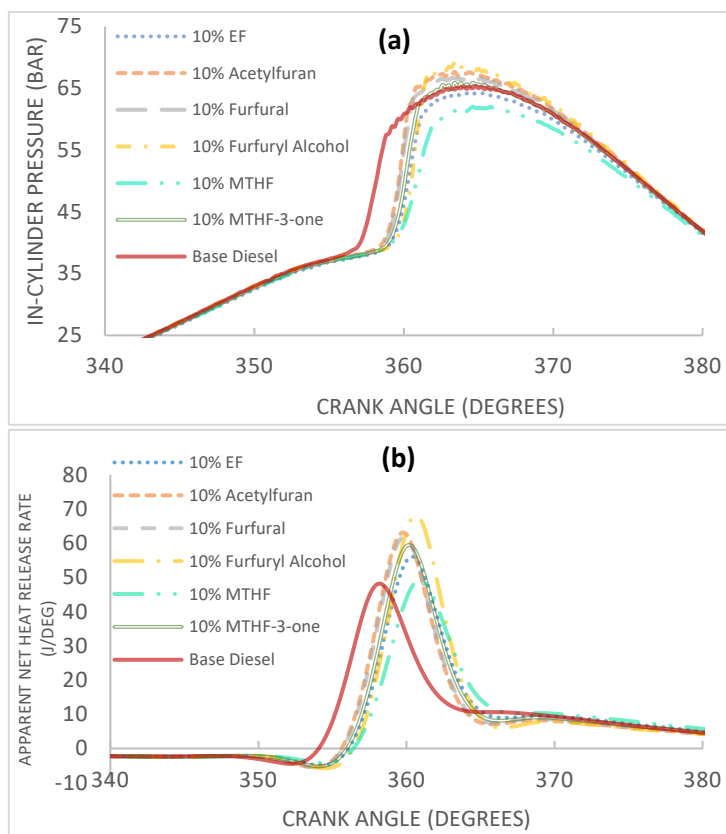
3.1.3. Effect of Oxygenated Side Chains

Figure 3.5: In-cylinder Pressure (a) and apparent net heat release rate (b) comparison of 70:20:10 diesel:butanol:furanic fuel blends, comparing various oxygenated functional groups

The trend between possessing different oxygenated functional groups is more subtle than that of the saturation or degree of branching; as can be seen in Figure 3.5, the most notable distinction is between the base diesel test and the blends, the latter of which are grouped. The readily visible longer ignition delay of the blends clearly allowed for a greater amount of premixed combustion and therefore a higher pHRR. Unlike the 50:50 blends, these blends consisted primarily of diesel (70 vol%), allowing pHRR to occur at approximately TDC (despite the likelihood of the furan component exhibiting undesirable combustion traits). Likely the main reason for only relatively minor differences between these blends is the fact that only 10% of the fuel was varied between each blend (as opposed to 50% of each blend in the previous tests). Despite this, there are some notable effects; in the case of furfural and furfuryl alcohol, a carbonyl group is replaced by an alcohol group and, while this may not seem a considerable change in 10% of the fuel, it is clear that the alcohol has an extended period of premixing,

555 indicated by the longer period before positive heat release and a greater premixed combustion

556 fraction.

557
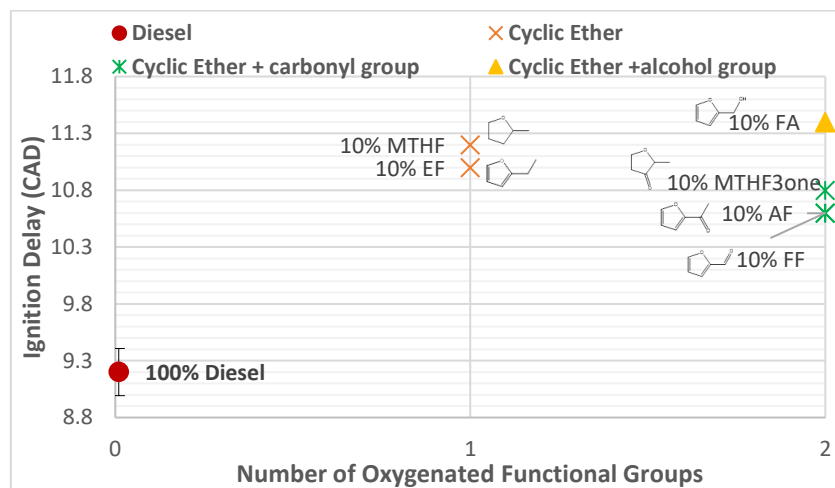
Figure 3.6: Duration of ignition delay, comparing various oxygenated functional groups within 70:20:10 diesel:butanol:furanic fuel blends and pure fossil diesel

559

560   Figure 3.6 shows that the ignition delay of furfural and acetylfuran, possessing two

561 oxygenated functional groups, exhibit a shorter delay time than ethylfuran, containing only a

562 single oxygen atom as an ether linkage within the aromatic ring. The same relationship is

563 shown when comparing saturated MTHF to MTHF-3-one, where the latter possesses an

564 additional oxygen atom in the form of a carbonyl group. However, furfuryl alcohol exhibited an

565 appreciably longer delay period than ethylfuran, highlighting the differing impact that dissimilar

566 oxygenated functional groups have on low temperature kinetics. In general, the delay period

567 of a straight chain oxygenated molecule is greater than that of straight chain hydrocarbon of

568 the same length.[49,50] The greater electronegativity of the oxygen atom (due to a greater proton

569 number compared to a carbon atom for the same number of orbitals) has a knock on effect

570 throughout the rest of the molecule, and therefore the bond dissociation energies of all C-H

571 bonds.

572   Ethylfuran possessed a longer ignition delay than acetylfuran (Figure 3.6); the latter is the

573 same structure as ethylfuran but with the addition of a carbonyl group on the first carbon on

574 the alkyl chain. Moreover, furfural also possessed a shorter delay period than ethylfuran,

575 despite, in the former, the loss of one carbon atom where hydrogen abstraction may occur

576 (and expected to reduce the delay period). A difference of 0.4 CAD in the delay period is not

577 substantial enough to draw any certain conclusions, but a decrease in ignition delay of the

578 same magnitude can also be noted when considering MTHF-3-one relative to MTHF, where

579 the change of molecular structure is- similarly- the addition of a carbonyl group (in this case

580 on the ring itself). Despite only a minor decrease in ID, it is significant that the delay period

581 does not increase, as one would anticipate with the addition of an oxygen atom. Furfuryl

582 alcohol, however, possess a significantly longer delay time than both ethylfuran and furfural.

583 This decrease in ignition delay from an alcohol to an aldehyde has been attributed to the high

584 reactivity of the latter species. Aldehydes are intermediates in the low temperature reactions

585 of alcohol, which essentially reduces the number of reaction stages required for complete

586 combustion of the oxygenated molecule. A further tentative suggestion here is that the delay

587 period of furfural is not increased, relative to single-carbon ethylfuran, because there is no

588 hydrogen connected to the additional oxygen in acetylfuran or furfural (the additional oxygen

589 is double bonded to the carbon only), while peroxy radicals are known to be easily formed

590 from these functional groups, increasing reactivity.[51] The same argument potentially explains

591 why the ignition delay period of furfuryl alcohol is significantly higher than furfural and

592 acetylfuran; a hydrogen atom is directly bonded to the oxygen on the alkyl chain. However,

593 when considering AF and FF relative to EF, one would assume a change in BDEs on the

594 remaining hydrogens in the molecule from the addition of a carbonyl group; Koivisto et. al[49]

595 studied a variety of carbonyl molecules in their propensity to ignite, finding that the ignition

596 delay increased between an alkane and a ketone of the same chain length. In the test blends

597 employed in the current study however, the molecule is predominantly cyclic rather than a

598 straight chain and, potentially, the additional oxygen has a more destabilising effect on the

599 overall molecule compared to ethylfuran. In essence, oxygens generally inhibit early stage

600 combustion reactions when added to straight chain alkanes, but appear to promote them when

601 added to aromatics and stable ring structures. The electron withdrawing effect of the

602 oxygenated side chain likely disrupts the π bonding that makes aromatic rings highly stable

603   and unreactive. Furthermore, it is important to note that hydrogen abstraction is not the only

604   process that dictates ignition delay; isomerization through chain branching is an important

605   pathway that increases the radical pool, and it has been shown that oxygenated species can

606   hinder this in straight chain molecules.[49] However, the change in the molecular characteristics,

607   created by the addition of a C=O bond to a furan, may enhance this relative to an alkylfuran.

608   Tetrahydrofurans (THFs) and furan differ in their aromaticity, Figure 3.6 shows that the

609   effect of a carbonyl group on ignition delay in both THF and furan ring structures is the same,

610   suggesting both ring structures are relatively stable species that can be disrupted by the

611   addition of an oxygen (carbonyl) group. In MTHF-3-one, the carbonyl group is directly

612   connected to the ring structure and, as in acetylfuran and furfural, this carbonyl group is not

613   connected to any hydrogens itself, therefore does not inhibit hydrogen abstraction from a

614   specific location. A further consideration is that, unlike in the case of furfuryl alcohol, hydrogen

615   bonding is not possible in the carbonyl (C=O) group molecules. This increase in intermolecular

616   force between molecules could also inhibit fuel atomisation and ignition; greater molecular

617   polarity tends to result in higher viscosities. In the case of MTHF-3-one, the carbonyl group

618   directly connected to the ring will likely alter the BDEs throughout the structure as it is a small

619   cyclic molecule. The electronegativity of the two oxygens on either side of the molecule will

620   draw electrons away from the centre of the molecule, plausibly making the hydrogens located

621   there more easily abstracted.

622

623   ### 3.1.4.   *Effect of Butanol*

624

625   MTHF and DMF were both used as 50:50 blended fuels with diesel and as 10% blends in

626   20% butanol and 70% diesel. This enabled comparisons to be made across the two ranges of

627   fuels tested, as well as the effect of butanol on the ignition and combustion characteristics to

628   be evaluated. The effect of butanol on diesel combustion relative to neat diesel is already well

629   established at a range of engine conditions, outlined in Babu's review,[52] however the current

630   study can give some insight into the effect of butanol on combustion relative to the furans

631 tested. Butanol as a diesel fuel extender has been shown to improve diesel combustion

632 characteristics to an extent.[52,53] However, high levels of butanol (greater than 40%[54]) lead to

633 long ignition delays due to the low cetane number of the alcohol, and so it was desirable that

634 the butanol concentration be minimised. The ratio of 70:20:10 was selected based on the

635 solubility of the furan fuels in diesel (for some of the molecules, double the amount of butanol

636 was required to successfully solvate the furan) rather than the applicability of butanol itself. A

637 further point to add is that, as can be seen in Table 2.4, the injection duration required to be

638 increased significantly during the 10% DMF and 10% MTHF blend tests. This suggests that

639 the butanol in particular possessed very poor lubricating properties, and the injection of fuel

640 was less consistent for these tests.
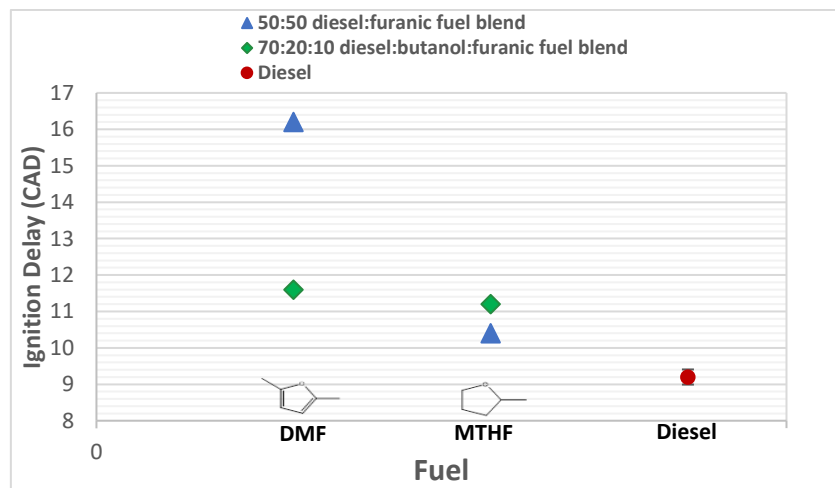
641

642 Figure 3.7: Comparison of the duration of ignition delay between DMF and MTHF 50:50 and 70:20:10 blends, as well as fossil diesel

643

644 Comparing the MTHF blends, Figure 3.7 illustrates that the ignition delay in the 50:50 blend

645 is slightly lower, which is positive when considering the applicability of these molecules as

646 fuels; despite the lower percentage of diesel in this blend, the propensity of this blend to ignite

647 was increased slightly when MTHF replaced butanol (and a percentage of the fossil diesel).

648 The opposite trend is observed when comparing 50 vol% DMF to 10 vol% DMF fuel and

649 20 vol% butanol. The 50:50 blend here possessed an extremely long ignition delay period of

650 over 16.2 CAD, whereas the 10% blend with additional butanol exhibited a delay period of

651 11.6 CAD. The additional diesel can help explain the shorter delay, but it is also possible the

652   butanol is having a positive effect relative to the DMF fraction it replaces. Overall, it can

653   reasonably concluded that, relative to butanol, MTHF has a greater propensity to ignite,

654   therefore a higher cetane than butanol (Sudholt calculated the cetane number of MTHF at

655   22,[21] while the derived cetane number of butanol is 15.92[37]) and hence can be considered,

656   along with other tetrahydrofurans, as a potential diesel blending component. However, fully

657   unsaturated furans, such as DMF (calculated cetane number of 10.9)[21] ignite poorly compared

658   to butanol. The very stable aromatic ring is difficult to break down in early stage combustion,

659   therefore its ignition delay is very high compared to butanol.

660

661   *3.2.   CO Emissions*
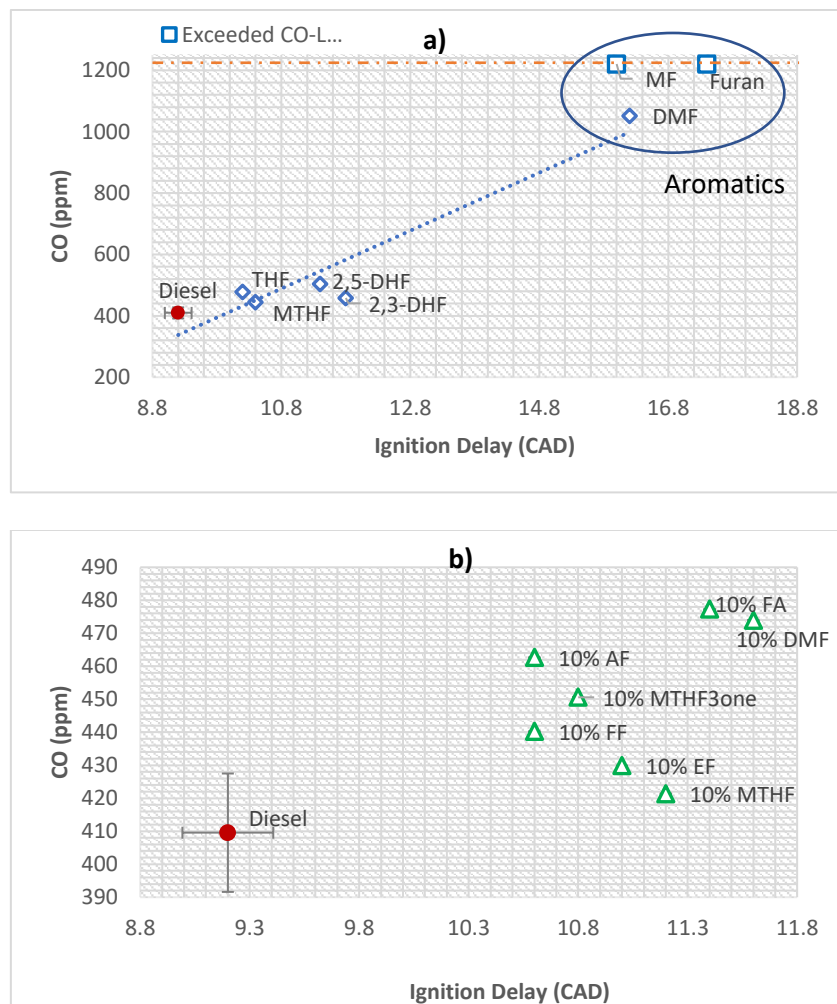
Figure 3.8: Exhaust CO levels (ppm) with varying ignition delay of a) 50:50 blends and b) 70:20:10 diesel:butanol blends

666

Figure 3.8 shows the CO emissions of the furan blends and reference diesel, relative to ignition delay. The emissions of CO are a strong indication of the degree to which complete combustion is occurring; higher CO emissions indicate more incomplete combustion.

Figure 3.8a indicates that the levels of CO emitted during the furan:diesel combustion were over twice as high as both DHFs and THF (the CO emissions of the furan:blend blend exceeded the CO upper detection threshold), suggesting that the combustion performance was very poor, in agreement with the late combustion phasing. It is pertinent to note the considerable jump in CO emissions, and therefore combustion efficiency, between the partially unsaturated DHFs and fully unsaturated furan; the CO emissions of 2,3-DHF were 20ppm lower than THF, despite the lower degree of saturation. The shorter ignition delay of THF could potentially result in higher levels of incomplete combustion products, relative to 2,3-DHF, due to lower levels of air premixing, potentially enhancing the presence of fuel-rich zones where CO is produced. This effect may have been slightly counteracted, however, if the ignition delay of the DHF blends was long enough for fuel to have become overdiluted; this could result in greater incomplete combustion due to the lower temperatures and quenching effect of the relatively cold cylinder walls, if fuel had become impinged here. This reasoning could also explain the lower CO emissions of pure diesel, which exhibited a shorter delay period than any of the blends yet. Despite the reduced time for air-fuel mixing, CO emissions are lower, thereby suggesting that overdilution in the extended premixing period is the primary mechanism of incomplete combustion.

Figures 3.8a also shows that unbranched furan and MF (one methyl branch) produced the highest CO emissions of all fuels tested (both exceeded the maximum threshold detectable, likely due to the very poor combustion quality exhibited by both (Figure 3.3), followed by DMF (two methyl branches), which produced approximately 40ppm higher CO emissions than EF (one ethyl branch) in the 10% blend tests (Figure 3.8b). This reinforces the conclusion that, among the furanic fuel blends tested, the levels of CO emitted do not follow the trend of reduced CO with shorter ignition delay. A further factor to consider is the magnitude and timing

694 of peak in-cylinder temperature. Figure 3.9 shows the magnitude and timing of the calculated

695 maximum in-cylinder global temperature for each of the blends tested. Apparent from Figure

696 3.9 are the higher temperatures attained when this peak occurs closer to TDC, earlier in the

697 expansion stroke.

698
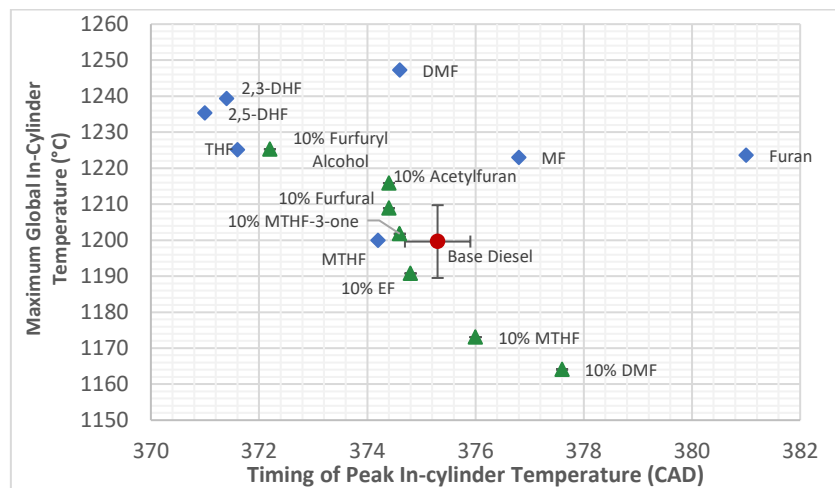
699

Figure 3.9: Magnitude and time of occurrence of calculated maximum in-cylinder temperature an of 50:50 furanic fuel:diesel blends and 70:20:10 diesel:butanol:furanic fuel blends

700

701 It can be seen from Figure 3.9 that furan exhibited a relatively late timing of peak in-cylinder

702 temperature compared to the other 50:50 diesel:furanic blends (and the lowest pHRR, as seen

703 in Figure 3.1b), and emitted higher levels of CO than all other fuels tested, with the potential

704 exception of the 50:50 MF:diesel blend (which also exceeded the CO detector threshold-

705 Figure 3.9). EF combustion meanwhile yielded higher cylinder temperatures than DMF in the

706 10% tests (the 10% DMF test saw the lowest peak temperatures of any blend) and slightly

707 lower CO emissions. Lower temperatures can be expected to cause increased incomplete

708 combustion and CO formation. Furan, MF and DMF displayed two stage combustion, as

709 shown in Figure 3.3b, whereby diesel reacts in the initial stage and the furan species only acts

710 initially as a diluent of the diesel, before being able to burn as the flame propagates (the flame

711 initiated by the diesel component). With these long ignition delays the fuel is likely to become

712 impinged on the cylinder walls, where temperatures are reduced relative to air-fuel mixture,

713 likely contributing to a further increase incomplete combustion products such as CO and

hydrocarbons. Figure 3.8a shows that between THF and MTHF, as with ignition delay (Figure

3.4), there is little difference in the level of CO emissions formed, most likely due to the similar

BDEs and reaction pathways of both of these molecules, despite the addition of a methyl

branch.

Figure 3.8b indicates that furfural and acetylfural blends exhibited higher CO emissions

than ethylfuran, following the trend of higher incomplete combustion products with a shorter

ignition delay and period for premixing. Figure 3.9 indicates that all of the oxygenated

alkylfurans (2 oxygen atoms within the structure) exhibited higher peak temperatures during

their combustion than ethylfuran, which could be due to pHRR occurring closer to TDC,

resulting in higher temperatures (indicated in Figure 3.9) through reduced heat transfer to

cylinder walls. The long ignition delay of the furfuryl alcohol blend did not result in a decrease

in CO emissions, which did not follow the same trend as that between ethylfuran, acetylfuran

and furfural blends. Furthermore, FA did not exhibit a low peak in-cylinder temperature that

could imply incomplete combustion (Figure 3.3b). In fact, the 70:20:10 DMF blend displayed

a longer delay period than FA (Figure 3.8), yet produced lower levels of CO (Figure 3.8b). The

physical properties of furfuryl alcohol therefore need to be considered; its density is much

higher compared to DMF, and its viscosity was noted to be higher when blending, which will

likely result in poorer atomization of the more dense and viscous alcohol and greater fuel

impingement on the cylinder walls. Further, this impinged fuel could be released in the

expansion stroke when it is not able to fully oxidise due to the lower temperatures present

during this combustion phase.

The physical properties of these different molecules can also help explain the difference

in CO emissions between the MTHF and MTHF-3-one blends. The shorter delay period in the

case of the latter would have reduced mixing time, thus resulting in larger fuel rich zones with

potential to form CO. However, given that the ignition delay difference is very small (Figure

3.6), it may not account for the increase in CO of MTHF-3-one shown in Figure 3.9b of 30

ppm. More likely, since MTHF-3-one was more viscous, the injection of this blend forms more

741   oxygen deficient zones, from reduced atomisation, where CO will form from incomplete

742   combustion.

743

744   *3.3.   NOx Emissions*

745
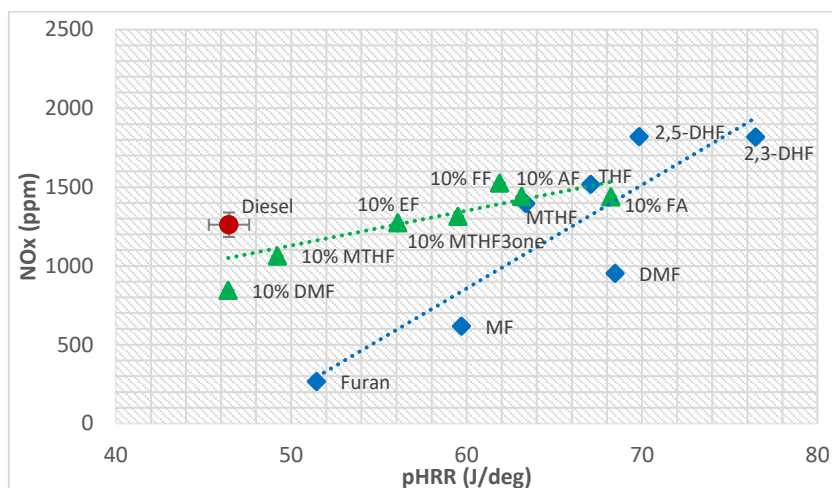
Figure 3.10: NOx emissions relative to peak heat release rates of 50:50 blends (blue diamond), 70:20:10 blends (green triangle) and fossil diesel (red circle)

748

749   Figure 3.10 shows the exhaust levels of NO_x for the furan blends and reference diesel,

750   relative to pHRR. Immediately apparent is the significantly lower level of NO_x emissions in the

751   case of the furan blend, relative to all other fuel blends tested, while the highest NO_x levels

752   were emitted by the partially saturated DHF blends. The levels of NO_x produced show a clear

753   trend of increasing with peak HRR. NO_x is predominantly formed via the thermal oxidation of

754   nitrogen, rates of which are strongly dependent on temperature, and this is also sensitive to

755   the duration for which sufficiently high temperatures are present. Considering the effect of

756   furan saturation, it can be seen that this causes a variation in NO_x levels predominantly through

757   the duration of ignition delay. The higher NO_x emissions in the case of DHF (Figure 3.10) are

758   postulated to be due to the longer ignition delay of the dihydrofurans compared to THF (Figure

759   3.4). However, the significantly prolonged ignition delay of the furan:diesel blend does not

760   elevate NO_x emissions due to a much later occurrence of maximum in-cylinder temperature

761 and ensuing poor combustion quality, as indicated by the observed high CO emissions (Figure

762 3.8).

763
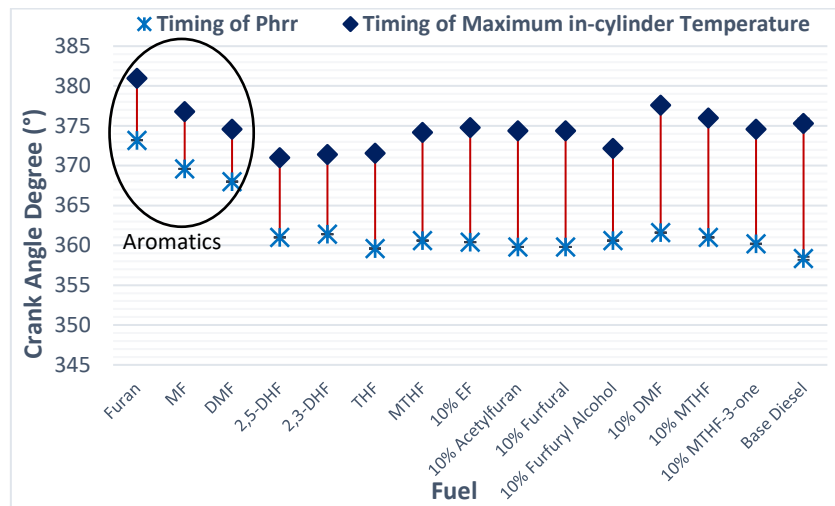
Figure 3.11: Timing of pHRR and peak in-cylinder temperatures of all blends

764

765

766

767   Combusting the furan:diesel blend likely resulted in conditions unsuitable to produce

768 substantial NO_x, as a result of the apparent quenching of diesel radical reactions resulting

769 from the presence of the aromatic furan molecule. From Figure 3.9, it can be seen that while

770 the calculated maximum in-cylinder temperature of the furan:diesel blend was comparable to

771 the other 50:50 blends tested, it occurred far later in the expansion stroke. It is suggested that,

772 despite sufficiently high maximum temperatures, due to rapid reductions in temperature during

773 the expansion stroke, these were present for too short a period of time for substantial NO_x to

774 be formed. Figure 3.11 demonstrates that peak heat release and peak temperatures occurred

775 far later in the furan blend compared to other blends, and illustrates that a longer duration

776 between pHRR and peak temperatures tends to result in higher NO_X. In the case of furan,

777 which emitted the lowest levels of NO_X, this duration is approximately 8 CAD, whereas for

778 fossil diesel the interval is 17 CAD. Therefore, despite furan combustion displaying a higher

779 peak temperature than diesel (Figure 3.9), it is the latter which produces higher NO_X emissions

780 (Figure 3.10).

781   Figure 3.10 clearly shows that, for the 50:50 diesel:furanic fuel blends, emissions of NO_x

782   increased as number of methyl branches attached to the aromatic ting increased (furan, MF

783   and DMF), with ethylfuran producing higher levels than DMF. NO_x output was, however,

784   comparable between THF and MTHF, within the margin of error indicated by the vertical error

785   bars of the diesel result. The higher NO_x emissions of DMF relative to MF can be likely

786   attributed to the higher in-cylinder maximum temperature observed in the case of the former

787   (Figure 3.10) and this is likewise the case when comparing ethylfuran to DMF and THF to

788   MTHF.

789   It can also be seen in Figure 3.10 that 70:20:10 diesel:butanol:furanic fuel blends

790   containing additional oxygen (AF, FF and FA) displayed higher NO_x emissions than ethylfuran.

791   This observation is consistent with the trends of peak heat release rate (Figure 3.5) and

792   maximum in-cylinder temperatures (Figure 3.9), with the exception of furfural, which emitted

793   levels of NO_x higher than furfuryl alcohol, despite a lower in-cylinder temperature. From Figure

794   3.11, it can be noted that the timings of pHRR and peak temperatures occur at almost identical

795   timings for the FF and FA blends, indicating that the longer delay of FA did not result in a

796   retarded release of energy. Longer delay periods tend to result in higher cylinder temperatures

797   as a result of greater duration for premixing, which can explain the higher temperatures during

798   furfuryl alcohol combustion compared to ethylfuran, but does not explain why acetylfuran and

799   furfural also produced higher temperatures than EF, since the delay period of these was

800   shorter (Figure 3.6). One tentative suggestion is that the greater density of more oxygenated

801   AF and FF (see Table 3.2) allows for more enhanced mixing rates due to greater spray

802   momentum, allowing for a greater premixed combustion phase that causes a higher pHRR.[55]

803   The additional oxygen may also account for the observed increase in the average cylinder

804   temperatures (Figure 3.6). The reason for this is twofold, firstly the adiabatic flame temperature

805   of oxygenated fuels tends to be higher[56] and, secondly, locally the combustion of these blends

806   may be more complete due to the increase in fuel-bound oxygen.

807   Figure 3.10 shows higher NO_x emissions from MTHF-3-one relative to MTHF, despite

808   comparable, if not shorter, ignition delay. This can likely be attributed to an earlier pHRR closer

809   to TDC (Figure 3.11) and, potentially, a greater rate of mixing in the case of the more dense

810   MTHF-3-one blend.[57]

811

812

813   *3.4.   Particulate emissions*

814
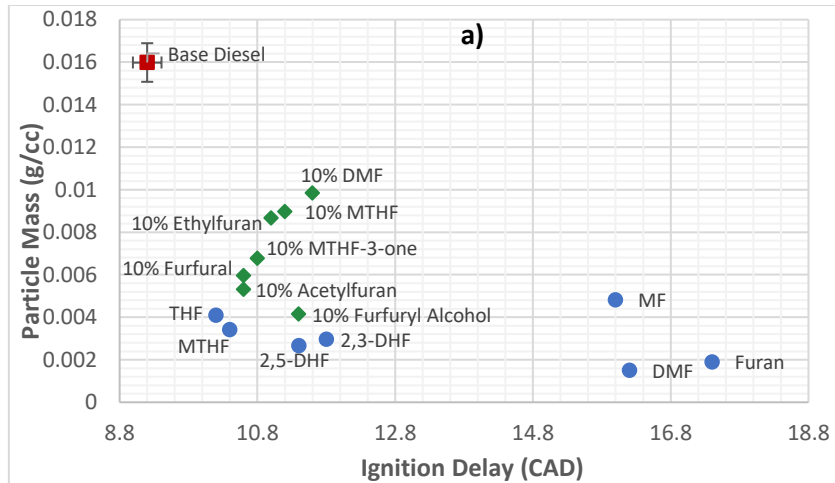
815
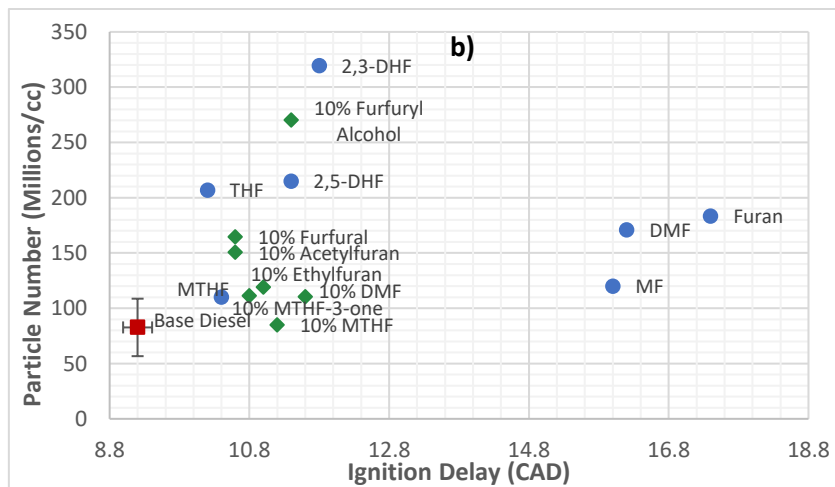
816

Figure 3.12: Exhaust emissions of a) Particle Mass and b) Particle Number of 50:50 blends (blue circle), 70:20:10 blends (green diamond) and diesel (red square), relative to ignition delay

817

818

819   Figure 3.12a and 3.12b show the total mass of particulate matter and total number of

820   particles emitted relative to the ignition delay of the 50:50 diesel:furanic fuel and 70:20:10

821   diesel:butanol blends. The most evident trend in Figure 3.12 is the difference between the

822   particulate output of the furanic blends and base diesel; the latter possesses a particle mass

823   a factor of four times greater than the furans, but a significantly lower particle number. It is

824   likely that the significant difference in ignition delay is the reason for this, as the onset of

825   combustion therefore begins earlier, allowing more time for particle formation and growth than

826   before the exhaust stroke, increasing particle mass while decreasing particle number

827   compared to the test blends. The shorter ignition delay during diesel combustion also leads to

828   the formation of more pyrolysis products in fuel rich zones within the combustion chamber,

829   therefore it is possible that there is a greater rate of soot formation initially. Moreover,

830   displacement of fossil diesel, which generally contains a significant proportion of aromatic and

831   unsaturated molecules, will likely have reduced the number of species that are able to readily

832   form soot; either through direct growth to larger aromatic species or via decomposition to short

833   chain unsaturated precursors.

834   There is evidently an effect of the degree of saturation on the particle mass emitted in the

835   exhaust, increasing from 0.00189 ug/cc, in the case of unsaturated furan, to 0.0041 ug/cc with

836   fully saturated THF, an amount greater than the indicated standard deviation error bars of the

837   observed PM emissions of diesel combustion across the testing period. The particulate mass

838   emitted by the DHF blends lies within this range (Figure 3.12a). THF possessed the shortest

839   delay period so, as with the CO emissions, there is less time for a homogenous fuel-air mixture

840   to be formed, and thus likely a greater presence of fuel rich zones that will likely form

841   particulates. In general, however, aromatic fuels are expected to produce greater particulate

842   mass, since aromatics themselves are soot precursors. Moreover, Karavalakis[58] notes that

843   aromatics are more difficult to vaporize than paraffins, meaning they are more susceptible to

844   becoming trapped on cylinder walls and in cylinder deposits. In the current study, an effect of

845   aromatics does not seem to be prevalent in increasing soot formation. These experiments

846   involve furan as the aromatic molecule, which contains oxygen; the presence of the oxygen in

847   the furan will potentially inhibit the formation of soot precursors; aromatic hydrocarbons that

848   are normally present in fossil diesel fuel- such as benzene- do not possess this oxygen and

849   likely form these precursors more easily. Substituting 50 vol% of the diesel is therefore

850   anticipated to result in a reduction in these known soot precursors. However, previous studies

851   have noted that furan is prone to forming acetylene- one of the building blocks for PAHs- while

852   DMF's major decomposition products include cyclopentadiene and benzene, which are also

853   precursors to particulates.[59] Alexandrino et. al noted that the formation of soot, and precursors

854   such as ethylene and acetylene, increased when using DMF relative to other oxygenated

855   fuels, such as ethanol or methyl formate.[60] However, the pyrolysis conditions used may not be

856   reflected in a combustion engine. Important to note also is the impact of engine load. Xiao[61]

857   conducted CI combustion studies into the use of DMF in diesel blends and noted that DMF

858   decreased 1,3-butadiene and benzene emissions, but increased acetaldehyde production.

859   However, engine load played a major part in the observations; at lower loads, DMF addition

860   decreased the concentration of soot but, at high engine loads (1.13MPa BMEP), the DMF

861   blends saw higher particle size distributions than pure diesel. It is suggested that, at lower

862   loads, the dilution of diesel is the dominant role of DMF while, at higher loads and

863   temperatures, DMF is able to contribute to the formation of soot in the mechanism explored in

864   more controlled pyrolysis studies by the likes of Alexandrino.[60,62]

865   In terms of particle mass (Figure 3.12a), there is little difference between the two

866   dihydrofurans, but 2,3-DHF produced a considerably higher particle number (Figure 3.12b),

867   greater than all other fuels tested. It is not clear why this occurs, but one could suggest the

868   2,3-DHF forms more soot later in combustion, relative to 2,5-DHF; these particles therefore

869   do not have time to grow in size due to the rapidly decreasing temperatures at this stage of

870   combustion. It has already been noted that the diesel seemingly dominates the early stage of

871   combustion in these blends (to a significant extent in the case of the furan:diesel blend) until

872   temperatures are high enough for the furanic component to also ignite (Figure 3.1b). Therefore

873   in the latter stages of a combustion cycle, the furanic molecule may dictate the formation of

874   particulates. Fan[43] notes that the reaction pathway of 2,5-DHF will initially yield stable furan,

875   which is less likely to form particulates, while 2,3-DHF produces large amounts of propene

876   and propene radicals, and these could be responsible for the formation of more soot

877   particles.[63] While THF produces greater particulate mass than both DHF molecules (Figure

878   3.12a), it produces fewer particles, suggesting these particles are generally larger, and this is

879   confirmed by the measured particle size distribution (see Supporting Information, Figure

880   A1(a)). One hypothesis is that there is potentially a greater degree of soot oxidation occurring

881   during the combustion of the dihydrofurans owing to the slightly higher in-cylinder

882   temperatures (Figure 3.9) relative to THF, which can be attributed to the longer ignition delay

883   of the former (Figure 3.2). Furthermore, since ignition (and thus combustion) occurs slightly

884   earlier in the THF:diesel blend relative to that of DHF, particles form earlier; the fuel spray is

885   less dispersed, there is more time for the particles formed to collide and grow into larger

886   particles via coalescence and agglomeration, and particle formation can occur when the piston

887   is closer to TDC at lower volume, and therefore higher density, making particle collisions more

888   likely.

889   The increase in branching of DMF compared to furan and MTHF compared to THF saw a

890   decrease in both particle mass and number. Figure 3.12 shows that the methylfuran blend

891   produced a greater particulate mass than either the furan or DMF blends, but the lowest

892   particle number of the full aromatic 50:50 blends. The trend in ignition delay (furan>

893   MF/DMF>EF) does not explain this result, and in this case the level of particulates formed

894   cannot be solely attributed to the amount of mixing allowed to occur before combustion

895   commences. Although, the higher soot emissions during MF combustion compared to DMF

896   could be attributed to overdilution and fuel impingement on the cylinder walls due to the

897   significantly extended ignition delay period of MF. The aforementioned poor combustion

898   quality of furan and methylfuran likely dominated the formation of particulates relative to other

899   fuels tested. The earlier injection timing of the furan blend (19 CAD BTDC) relative to MF (17

900   CAD BTDC) could explain the significantly higher particulate mass produced by methylfuran

901   compared to furan (Figure 3.12a). The peak temperatures reached during combustion of both

902   blends were very similar (Figure 3.9), but this temperature occurred earlier with the MF:diesel

903   (Figure 3.11). With in-cylinder temperatures being higher earlier in the expansion stroke, more

904   fuel would have been available to pyrolyse and form soot, relative to furan:diesel combustion.

905   Comparing DMF and EF, the latter emitted slightly lower particulate mass in the 70:20:10

906   blends (Figure 3.12a). This is likely due to the very long delay period shown by the DMF blend

907   (Figure 3.6), which may have resulted in overmixing, which concurs with the CO emission

908   observed (Figure 3.9b). The higher particle number exhibited by ethylfuran (Figure 3.12b)

909   suggests that the particles emitted from the DMF:butanol:diesel blend were larger (indicated

910   in Figure A1(b) in the Appendix), and potentially formed earlier. In addition to overdilution, it is

911   suggested that the molecular structure of DMF could be responsible for the relatively higher

912   emission of particulates compared to EF. Hoang et. al reviewed the current knowledge of DMF

913   combustion, outlining that unimolecular decomposition is a major pathway in the breakdown

914   of the molecule, with initial bond breaking at the C-H site on the methyl carbons and

915   subsequent ring-opening resulting in 1,3-butadiene as a major product, a well-known soot

916   precursor.[64] A study by Song meanwhile described the main products of EF decomposition as

917   primarily 2-vinylfuran, 2-furylmethyl and vinylketene, and suggest that the hydrocarbons

918   formed in the pyrolysis of DMF are more likely to form soot precursors.[65]

919   An appreciable difference in particulate mass emissions between THF and MTHF can be

920   seen in Figure 3.12; the THF blend produced 0.0041 ug/cc, while MTHF produced 0.0034

921   ug/cc. This could partially be explained by the slightly shorter delay period observed for THF

922   (Figure 3.4). However, since the difference in ID is only small, other explanations are

923   warranted. Some of the trends noted in these experiments could potentially be explained by

924   the difference in volatility between molecules. A more volatile fuel (the boiling point of THF is

925   66°C, while the boiling point of MTHF is 80.2°C) could result in a fuel vapour cloud forming

926   close to the injector nozzle, which will create local temperature hot spots in this area and high

927   soot formation due to the relatively fuel rich zone.

928   Figure 3.12a also shows that the mass of particulates was consistently lower for the

929   molecules with greater oxygen content. This oxygen will play a role in the particulates'

930   oxidation phase, while the higher temperatures exhibited in the combustion of these fuels

931   would enhance oxidation rates further compared to ethylfuran. Furfuryl alcohol combustion

932   displayed the lowest particle mass overall; acetylfuran and furfural blends produced slightly

933   higher PM emissions, though less than EF. This could suggest a greater ability for oxygen

934   bonded to carbon and hydrogen to aid in the oxidation of soot particles, as is the case in

935   alcohols. The C=O bond is difficult to break, whereas oxygen in the alcohol likely becomes

936   more readily available for oxidation earlier during combustion. The particulate number exhibits

937   the opposite trend, whereby the lowest particulate number is emitted by the DMF blend (1

938   oxygen atom), while the highest is found in furfuryl alcohol combustion. Hellier et. al[25] reviewed

939   the effect of various oxygenated functional groups on soot formation, and concluded that the

940   carbon bonded to the oxygen in a ketone group did not contribute to soot formation, while the

941   carbon connected to a hydroxyl group in an alcohol was involved in particulate formation. So,

942   while particulate mass decreased due to enhanced oxidation in FA, it is suggested that this

943   blend formed more soot initially, thus a greater number of particles were detected. Both FA

944   and DMF possessed a very long delay period in which fuel impingement may occur, but the

945   particle number was considerably lower in the case of DMF combustion (Figure 3.12b). The

946   reason for this is potentially due to the poorer combustion quality exhibited when using the

947   DMF blend; furan itself is an aromatic that is difficult to open, and DMF does not possess any

948   polar groups that can destabilise the ring and significantly inhibit this effect. Furthermore,

949   temperatures appeared far higher during furfuryl alcohol blend combustion compared to the

950   DMF blend (Figure 3.9), which would likely promote the initial formation of the pyrolysis

951   products. Physical properties of these molecules also need to be considered. The greater

952   hydrogen bonding of furfuryl alcohol, compared to DMF, can be reasonably expected to

953   increase blend viscosity, an attribute that reduces air entrainment and fuel atomisation, leading

954   to larger fuel droplets and, therefore, more localised pyrolysis zones to form soot.

955   The delay period of furfural/acetylfuran was similar to that of ethylfuran, but the more

956   oxygenated former species produced a higher particulate number. This could also be

957   attributed to the increased viscosity of these fuels that make atomization more difficult and

958   therefore fuel rich zones more prevalent. Meanwhile, the higher cylinder temperatures during

959   AF/FF/FA combustion, relative to EF, could also result in higher levels of soot being formed

960   initially (due to an enhanced kinetic effect) before these oxygenated alkylfurans see an

961 enhanced oxidation phase and considerably reduce the particulate mass. The same

962 explanations can explain the apparent trend when comparing MTHF and MTHF-3-one; the

963 fuel with greater fuel-bound oxygen (MTHF-3-one), greater viscosity and maximum calculated

964 peak in-cylinder temperatures, produces lower levels of particulates on a mass basis,

965 approximately 0.0068ug/cc compared to 0.009ug/cc (Figure 3.12a).

966   A final consideration is the increase in boiling points noted in the more oxygenated species

967 (Table 2.3). For example, the boiling point of FA is 170°C, whereas the boiling point of DMF

968 is just 92°C. Considering the boiling point of butanol- 118°C - the blend of diesel, butanol and

969 FA contains components of vastly different volatilities. It has been shown that ternary blends

970 of this type undergo micro-explosions, a phenomenon in which a volatile fuel component

971 (butanol in this instance) becomes trapped inside the bulk fuel droplets, superheating to form

972 bubbles that eventually 'explode' and disperse the parent fuel droplet.[57,66] This aids in fuel

973 atomisation, reducing fuel-rich zones and thus could help account for the reduction in particle

974 mass seen in more oxygenated furanic fuel blends. It is also suggested that, in addition to

975 physical fuel effects and fuel bound oxygen causing an increase in soot oxidation, oxygen

976 atoms could inhibit stages of soot formation by disrupting aromatic ring growth on a molecular

977 level. Isotope tracing experiments have indicated that carbons bonded to oxygen atoms are

978 less likely to be involved in soot formation- forming CO and CO_2 more readily- while the

979 increase in potential species, such as OH radicals, available due to an increase in oxygen

980 content, has been indicated to limit PAH growth.[67,68]

981

982 **4. Conclusions**

983

984   The screening of the various biomass-derived molecules as blends with diesel and butanol

985 has helped to determine viable bio-derived molecules that could be investigated more

986 extensively, with the following specific conclusions drawn.

987   1. The ring structure of the bioderived molecule needed to be saturated, or at least

988   only partially unsaturated, for stable combustion and to avoid excessively long

989 durations of the ignition delay period. The long ignition delay of aromatic furan, MF

990 and DMF 50:50 blends, meant combustion occurred very late in the expansion

991 stroke.

992 2. The long ignition delay of blends containing stable aromatic species was not only

993 detrimental to the overall combustion quality (observed by the high carbon

994 monoxide emissions of these blends) but also meant that soot was formed very

995 late, allowing less time for soot oxidation, resulting in a high particulate number.

996 3. This late combustion also meant that temperatures required for thermal NO_x

997 formation were not attained for a significant duration, therefore furan, MF and DMF

998 blends produced the lowest of these emissions of all fuels tested.

999 4. The greater ignition quality of EF relative to DMF suggests that the presence of two

1000 carbons within an alkyl chain is particularly beneficial to the ignition quality of a

1001 cyclic molecule. Comparing THF to MTHF; the addition of one carbon to the ring

1002 did not make a notable difference to ignition delay or the resulting emissions of CO

1003 or NO_x, suggesting future tests should look into the use of longer alkyl chains from

1004 a ringed structure.

1005 5. The addition of a carbonyl group to the furan/THF structure was observed to

1006 shorten the ignition delay, increase CO and NO_x emissions, while decreasing the

1007 particle mass and increasing particle number. Alcohol group addition to a

1008 furan/THF molecule exacerbated these trends compared to the carbonyl group,

1009 producing even lower emissions of CO and particle mass (and a higher number).

1010 An extended ignition delay and impact on the fuel physical properties of the alcohol

1011 potentially explains this trend, as well as the fact that alcohols are more effective

1012 in oxidising particles than carbonyl equivalents.

1013 6. All test blends displayed the same trait in particulate emissions (decreasing mass

1014 and increasing number). The substitution of a significant vol% of diesel is likely the

1015 major cause at these load conditions, as the hydrocarbons present in diesel are

1016 prone to forming soot in fuel rich zones of the fuel jet. However, it has been shown

1017   that DMF, for example, also forms soot precursors during thermal decomposition.[15]

1018   Therefore, other factors, such as the presence of fuel-bound oxygen and an

1019   extended ignition delay (causing a reduction in the time available for particle

1020   formation and growth) could contribute to this trend.

Nomenclature and Units

AF = Acetylfuran

ATDC = After top-dead centre

BSFC = Brake-specific fuel consumption

BTDC = Before top-dead centre

CAD = Crank angle degree (°)

CI = Compression ignition

CO = Carbon monoxide

CO_2 = Carbon dioxide

COV = Coefficient of variation

2,3-DHF = 2,3-Dihydrofuran

2,5-DHF = 2,5-Dihydrofuran

DMF = Dimethylfuran

EF = Ethylfuran

FA= Furfuryl Alcohol

FF = Furfural

H_2= Hydrogen

H_2O = Water

HRR = Heat release rate (J/degree)

ICE = Internal combustion engine

ID = Ignition delay (CAD)

IMEP = Indicated mean effective pressure (bar)

MF = Methylfuran

MTHF = Methyltetrahydrofuran

MTHF-3-one = 2-Methyltetrahydrofuran-3-one

N_2 = Nitrogen

IR = Infrared Radiation

O_2 = Oxygen

ppm= Parts per million

NO_x = Nitrous oxides

pHRR= Peak heat release rate (J/deg)

PM = Particle mass (ug/cc)

PN = Particle number (N/cc)

SI = Spark ignition

SOC = Start of combustion

SOI = Start of injection

TDC= Top dead centre

UHC= Unburnt hydrocarbons

References

1. Geng, P., Cao, E., Tan, Q. & Wei, L. Effects of alternative fuels on the combustion characteristics and emission products from diesel engines: A review. *Renewable and Sustainable Energy Reviews* (2017). doi:10.1016/j.rser.2016.12.080

2. Furuholt, E. Life cycle assessment of gasoline and diesel. *Resour. Conserv. Recycl.* (1995). doi:10.1016/0921-3449(95)00020-J

3. Dhal, G. C., Mohan, D. & Prasad, R. Preparation and application of effective different catalysts for simultaneous control of diesel soot and NO $_X$ emissions: An overview. *Catal. Sci. Technol.* (2017). doi:10.1039/C6CY02612E

4. Colsa, A. *DIRECTORATE GENERAL FOR INTERNAL POLICIES Comparative study on the differences between the EU and US legislation on emissions in the automotive sector.* (2016).

5. Bergthorson, J. M. & Thomson, M. J. A review of the combustion and emissions properties of advanced transportation biofuels and their impact on existing and future engines. *Renewable and Sustainable Energy Reviews* (2015). doi:10.1016/j.rser.2014.10.034

6. Heywood, J. . *Internal Combustion Engine Fundamentals.* (McGraw-Hill Inc, 1988).

7. Menon, V. & Rao, M. Trends in bioconversion of lignocellulose: Biofuels, platform chemicals & biorefinery concept. *Progress in Energy and Combustion Science* (2012). doi:10.1016/j.pecs.2012.02.002

8. Rezania, S. *et al.* Review on transesterification of non-edible sources for biodiesel production with a focus on economic aspects, fuel properties and by-product applications. *Energy Conversion and Management* **201**, (2019).

9. Climent, M. J., Corma, A. & Iborra, S. Conversion of biomass platform molecules into fuel additives and liquid hydrocarbon fuels. *Green Chemistry* (2014). doi:10.1039/c3gc41492b

10.   Lange, J. P., Van Der Heide, E., Van Buijtenen, J. & Price, R. Furfural-A promising platform for lignocellulosic biofuels. *ChemSusChem* (2012). doi:10.1002/cssc.201100648

11.   Kläusli, T. AVA Biochem: commercialising renewable platform chemical 5-HMF. *Green Process. Synth.* (2014). doi:10.1515/gps-2014-0029

12.   Corma, A., De La Torre, O. & Renz, M. Production of high quality diesel from cellulose and hemicellulose by the Sylvan process: Catalysts and process variables. *Energy Environ. Sci.* (2012). doi:10.1039/c2ee02778j

13.   Corma, A., De La Torre, O., Renz, M. & Villandier, N. Production of high-quality diesel from biomass waste products. *Angew. Chemie - Int. Ed.* (2011). doi:10.1002/anie.201007508

14.   Corma, A., Delatorre, O. & Renz, M. High-quality diesel from hexose- and pentose-derived biomass platform molecules. *ChemSusChem* (2011). doi:10.1002/cssc.201100296

15.   Eldeeb, M. & Akih-Kumgeh, B. Recent Trends in the Production, Combustion and Modeling of Furan-Based Fuels. *Energies* (2018). doi:10.3390/en11030512

16.   Nguyen, D. C. *et al.* A review on the performance, combustion, and emission characteristics of spark-ignition engine fueled with 2,5-dimethylfuran compared to ethanol and gasoline. *J. Energy Resour. Technol. Trans. ASME* **143**, (2021).

17.   Xiao, H., Zeng, P., Li, Z., Zhao, L. & Fu, X. Combustion performance and emissions of 2-methylfuran diesel blends in a diesel engine. *Fuel* (2016). doi:10.1016/j.fuel.2016.02.006

18.   Gogoi, B. *et al.* Effects of 2,5-dimethylfuran addition to diesel on soot nanostructures and reactivity. *Fuel* (2015). doi:10.1016/j.fuel.2015.07.038

19.   Alexandrino, K. Comprehensive Review of the Impact of 2,5-Dimethylfuran and 2-Methylfuran on Soot Emissions: Experiments in Diesel Engines and at Laboratory-Scale. *Energy and Fuels* **34**, (2020).

20.   Hoang, A. T., Ölçer, A. I. & Nižetić, S. Prospective review on the application of biofuel

2,5-dimethylfuran to diesel engine. *Journal of the Energy Institute* **94**, (2021).

21. Sudholt, A. *et al.* Ignition characteristics of a bio-derived class of saturated and unsaturated furans for engine applications. *Proc. Combust. Inst.* (2015). doi:10.1016/j.proci.2014.06.147

22. De Bruycker, R. *et al.* Experimental and modeling study of the pyrolysis and combustion of 2-methyl-tetrahydrofuran. *Combust. Flame* **176**, (2017).

23. Wang, J., Wang, X., Fan, X., Yang, K. & Zhang, Y. An ignition delay time and kinetic study of 2-methyltetrahydrofuran at high temperatures. *Fuel* (2016). doi:10.1016/j.fuel.2016.08.104

24. Jouzdani, S., Eldeeb, M. A., Zhang, L. & Akih-Kumgeh, B. High-Temperature Study of 2-Methyl Furan and 2-Methyl Tetrahydrofuran Combustion. *Int. J. Chem. Kinet.* (2016). doi:10.1002/kin.21008

25. Hellier, P., Talibi, M., Eveleigh, A. & Ladommatos, N. An overview of the effects of fuel molecular structure on the combustion and emissions characteristics of compression ignition engines. *Proc. Inst. Mech. Eng. Part D J. Automob. Eng.* (2017). doi:10.1177/0954407016687453

26. Alipour, S., Omidvarborna, H. & Kim, D. S. A review on synthesis of alkoxymethyl furfural, a biofuel candidate. *Renewable and Sustainable Energy Reviews* (2017). doi:10.1016/j.rser.2016.12.118

27. Yang, F. *et al.* A biodiesel additive: Etherification of 5-hydroxymethylfurfural with isobutene to tert-butoxymethylfurfural. *Catal. Sci. Technol.* (2015). doi:10.1039/c5cy00750j

28. de Jong, E. & Gruter, G.-J. Furanics: A Novel Diesel Fuel with Superior Characteristics. in (2009). doi:10.4271/2009-01-2767

29. Omidvarborna, H., Kumar, A. & Kim, D. S. Variation of diesel soot characteristics by different types and blends of biodiesel in a laboratory combustion chamber. *Sci. Total Environ.* (2016). doi:10.1016/j.scitotenv.2015.11.076

30. Hellier, P., Ladommatos, N. & Yusaf, T. The influence of straight vegetable oil fatty

acid composition on compression ignition combustion and emissions. *Fuel* (2015). doi:10.1016/j.fuel.2014.11.021

31.   Pelucchi, M., Cavallotti, C., Ranzi, E., Frassoldati, A. & Faravelli, T. Relative Reactivity of Oxygenated Fuels: Alcohols, Aldehydes, Ketones, and Methyl Esters. *Energy and Fuels* (2016). doi:10.1021/acs.energyfuels.6b01171

32.   Zhang, Z. H. & Balasubramanian, R. Investigation of particulate emission characteristics of a diesel engine fueled with higher alcohols/biodiesel blends. *Appl. Energy* (2016). doi:10.1016/j.apenergy.2015.10.173

33.   Wang, C. *et al.* Combustion characteristics and emissions of 2-methylfuran compared to 2,5-dimethylfuran, gasoline and ethanol in a DISI engine. in *Fuel* (2013). doi:10.1016/j.fuel.2012.05.043

34.   Sharma, M., Sharma, P. & Kim, J. N. Solvent extraction of aromatic components from petroleum derived fuels: A perspective review. *RSC Advances* **3**, 10103–10126 (2013).

35.   Kittelson, D. & Kraft, M. Particle Formation and Models in Internal Combustion Engines. (2014).

36.   Frenklach, M. Reaction mechanism of soot formation in flames. *Phys. Chem. Chem. Phys.* **4**, 2028–2037 (2002).

37.   Lapuerta, M., Hernández, J. J., Fernández-Rodríguez, D. & Cova-Bonillo, A. Autoignition of blends of n-butanol and ethanol with diesel or biodiesel fuels in a constant-volume combustion chamber. *Energy* (2017). doi:10.1016/j.energy.2016.10.090

38.   Sigma Aldrich (Product Properties). Available at: www.sigmaaldrich.com/.

39.   Dahmen, M. & Marquardt, W. A Novel Group Contribution Method for the Prediction of the Derived Cetane Number of Oxygenated Hydrocarbons. *Energy and Fuels* (2015). doi:10.1021/acs.energyfuels.5b01032

40.   Buckingham, G. T. & Carleton, B. A. *PYROLYSIS AND SPECTROSCOPY OF CYCLIC AROMATIC COMBUSTION INTERMEDIATES*. (2010).

41.   Boot, M. D., Tian, M., Hensen, E. J. M. & Mani Sarathy, S. Impact of fuel molecular structure on auto-ignition behavior – Design rules for future high performance gasolines. *Progress in Energy and Combustion Science* (2017). doi:10.1016/j.pecs.2016.12.001

42.   Jenkins, R. W. *et al.* The Effect of Functional Groups in Bio-Derived Fuel Candidates. *ChemSusChem* (2016). doi:10.1002/cssc.201600159

43.   Fan, X., Wang, X., Wang, J. & Yang, K. Comparative Shock Tube and Kinetic Study on High-Temperature Ignition of 2,3-Dihydrofuran and 2,5-Dihydrofuran. doi:10.1021/acs.energyfuels.6b01332

44.   Eldeeb, M. A. & Akih-Kumgeh, B. Investigation of 2,5-dimethyl furan and iso-octane ignition. *Combust. Flame* (2015). doi:10.1016/j.combustflame.2015.02.013

45.   Grela, M. A., Amorebieta, V. T. & Colussi, A. J. Very low pressure pyrolysis of furan, 2-methylfuran, and 2,5-dimethylfuran. The stability of the furan ring. *J. Phys. Chem.* (1985). doi:10.1021/j100247a011

46.   Liu, D. *et al.* Combustion chemistry and flame structure of furan group biofuels using molecular-beam mass spectrometry and gas chromatography - Part I: Furan. *Combust. Flame* (2014). doi:10.1016/j.combustflame.2013.05.028

47.   Tran, L. S. *et al.* Combustion chemistry and flame structure of furan group biofuels using molecular-beam mass spectrometry and gas chromatography - Part II: 2-Methylfuran. *Combust. Flame* (2014). doi:10.1016/j.combustflame.2013.05.027

48.   Togbé, C. *et al.* Combustion chemistry and flame structure of furan group biofuels using molecular-beam mass spectrometry and gas chromatography - Part III: 2,5-Dimethylfuran. *Combust. Flame* (2014). doi:10.1016/j.combustflame.2013.05.026

49.   Koivisto, E., Ladommatos, N. & Gold, M. Compression Ignition and Exhaust Gas Emissions of Fuel Molecules Which Can Be Produced from Lignocellulosic Biomass: Levulinates, Valeric Esters, and Ketones. *Energy and Fuels* (2015). doi:10.1021/acs.energyfuels.5b01314

50.   Koivisto, E., Ladommatos, N. & Gold, M. Systematic study of the effect of the hydroxyl

functional group in alcohol molecules on compression ignition and exhaust gas emissions. *Fuel* (2015). doi:10.1016/j.fuel.2015.03.042

51.   Hellier, P., Al-Haj, L., Talibi, M., Purton, S. & Ladommatos, N. Combustion and emissions characterization of terpenes with a view to their biological production in cyanobacteria. *Fuel* (2013). doi:10.1016/j.fuel.2013.04.042

52.   Vinod Babu, V. B. M., Madhu Murthy, M. M. K. & Amba Prasad Rao, G. Butanol and pentanol: The promising biofuels for CI engines – A review. *Renewable and Sustainable Energy Reviews* (2017). doi:10.1016/j.rser.2017.05.038

53.   Rakopoulos, D. C. *et al.* Investigation of the performance and emissions of bus engine operating on butanol/diesel fuel blends. *Fuel* (2010). doi:10.1016/j.fuel.2010.03.047

54.   Rajesh Kumar, B. & Saravanan, S. Use of higher alcohol biofuels in diesel engines: A review. *Renewable and Sustainable Energy Reviews* (2016). doi:10.1016/j.rser.2016.01.085

55.   Liu, J. *et al.* Effects of diesel/PODE (polyoxymethylene dimethyl ethers) blends on combustion and emission characteristics in a heavy duty diesel engine. *Fuel* (2016). doi:10.1016/j.fuel.2016.03.019

56.   Koivisto, E. *Ignition and combustion of future oxygenated fuels in compression-ignition engines.* (2015).

57.   Zhang, P. *et al.* Spray, atomization and combustion characteristics of oxygenated fuels in a constant volume bomb: A review. *Journal of Traffic and Transportation Engineering (English Edition)* (2020). doi:10.1016/j.jtte.2020.05.001

58.   Karavalakis, G. *et al.* Evaluating the effects of aromatics content in gasoline on gaseous and particulate matter emissions from SI-PFI and SIDI vehicles. *Environ. Sci. Technol.* (2015). doi:10.1021/es5061726

59.   Eldeeb, M. A. & Akih-Kumgeh, B. Reactivity trends in furan and alkyl furan combustion. *Energy and Fuels* (2014). doi:10.1021/ef501181z

60.   Alexandrino, K., Millera, Á., Bilbao, R. & Alzueta, M. U. Novel aspects in the pyrolysis and oxidation of 2,5-dimethylfuran. *Proc. Combust. Inst.* (2015).

doi:10.1016/j.proci.2014.06.002

61. Xiao, H., Hou, B., Zeng, P. & Jiang, A. Combustion and emissions characteristics of a diesel engine fueled with blends of diesel and DMF. *Kexue Tongbao/Chinese Sci. Bull.* (2017). doi:10.1360/N972017-00020

62. Alexandrino, K., Salvo, P., Millera, Á., Bilbao, R. & Alzueta, M. U. Influence of the Temperature and 2,5-Dimethylfuran Concentration on Its Sooting Tendency. *Combust. Sci. Technol.* (2016). doi:10.1080/00102202.2016.1138828

63. Westbrook, C. K., Pitz, W. J. & Curran, H. J. Chemical kinetic modeling study of the effects of oxygenated hydrocarbons on soot emissions from diesel engines. *J. Phys. Chem. A* (2006). doi:10.1021/jp056362g

64. Hoang, A. T., Nizetic, S., Olcer, A. . & Ong, H. C. Synthesis pathway and combustion mechanism of a sustainable biofuel 2,5-Dimethylfuran: Progress and prospective. *Fuel* **286**, (2021).

65. Song, S. *et al.* Experimental and kinetic modeling studies of 2-ethylfuran pyrolysis at low and atmospheric pressures. *Combust. Flame* **226**, 430–444 (2021).

66. Liu, Y., Li, J., Gao, Y. & Yuan, X. Analysis of micro-explosion phenomenon in a constant volume chamber by butanol-biodiesel-diesel blend fuel. in *Advanced Materials Research* (2012). doi:10.4028/www.scientific.net/AMR.443-444.996

67. Cheng, A. S., Dibble, R. W. & Buchholz, B. A. The Effect of Oxygenates on Diesel Engine Particulate Matter. in (2002). doi:10.4271/2002-01-1705

68. Eveleigh, A. & Ladommatos, N. Isotopic Tracers for Combustion Research. *Combustion Science and Technology* (2017). doi:10.1080/00102202.2016.1246440